

**UNIVERSITY OF MANITOBA SOCIETY OF AUTOMOTIVE ENGINEERS**

DOCUMENT PREPARED FOR:

PROFESSOR P. E. LABOSSIERE  
DEPARTMENT OF MECHANICAL ENGINEERING  
UNIVERSITY OF MANITOBA  
PROJECT ADVISOR



**DESIGN OF AN ENGINE TEST STAND  
DESIGN REPORT**

**SUBMITTED:**  
2010-12-06

**Prepared by Team 18:**

ANDREW OLDENKAMP

BAHAE OMID

COURTNEY SKENE-HAMILTON

KELLY EGILSON

Andrew Oldenkamp

2010-12-06

Professor P. E. Labossiere  
Department of Mechanical Engineering  
Faculty of Engineering  
University of Manitoba  
Winnipeg, Manitoba  
R3T 2N2

Dear Professor Labossiere,

Please find attached the design report entitled "Design of an Engine Test Stand." This report has been submitted on December 06, 2010 by Team 18 of section A01. Team 18 consists of Andrew Oldenkamp, Bahae Omid, Courtney Skene-Hamilton and Kelly Egilson.

The purpose of the report is to present the design of an engine test stand. This report will touch on the methodology and development stages of the project, including the background the project objectives. The details of the design as well as a full outline of the design are also presented including costs and engineering specifications for implementation of the design.

Sincerely,

Andrew Oldenkamp  
Team 18 leader

Enclosure

## **ABSTRACT**

The primary purpose of this design project is to develop a test stand for a two-stroke model aircraft engine that is capable of measuring thrust and torque simultaneously and independently. The test stand will be designed for the University of Manitoba Aero Team in order to obtain accurate performance data for a more successful result in the annual competitions. Previous studies, which have included patents and journal articles, have dealt with the measurement of either the thrust or the torque. The proposed test stand takes advantage of a mechanism that achieves the simultaneous and independent measurement of both quantities. The mechanism involves using a two-piece test stand that decouples the effect of the thrust and torque by means of a bearing shaft connected to the engine mounting plate. The quantities of interest will be measured autonomously using the conventional strain gage based contact method. Various alternative designs were considered in the process of the concept development. The designs were studied independently and the final design was proposed through optimization and was based on the client's needs and specifications. Analytical modeling and several physical tests were conducted to assess the strength and effectiveness of the test stand. In conclusion, the study has found that the proposed test stand featuring robustness, portability, adaptability, and reliability best suits the client's needs and is a feasible and practical solution to the requirements.

## TABLE OF CONTENTS

	<b>page</b>
LIST OF FIGURES.....	III
LIST OF TABLES.....	IV
I. INTRODUCTION .....	1
A. PROJECT OBJECTIVES AND SCOPE .....	2
B. TARGET SPECIFICATIONS .....	5
II. DESIGN .....	6
A. FEATURES OF THE DESIGN .....	6
B. PRODUCTION AND ASSEMBLY DRAWINGS.....	10
C. TEST STAND OPERATION.....	13
D. OVERALL COST AND BILL OF MATERIALS.....	19
III. CONCLUSIONS .....	23
IV. REFERENCES .....	25
APPENDICES .....	28
APPENDIX A. CONCEPT DEVELOPMENT.....	28
APPENDIX B. NON-CONTACT SENSORS .....	34
APPENDIX C. TECHNICAL ANALYSIS AND VALIDATION .....	41
1. SIZING OF THE DEFLECTION ARM .....	41
2. SIZING OF THE THRUST SENSOR .....	44
3. LINEAR BEARING FRICTION TESTING AND ANALYSIS.....	46
4. SIZING OF THE BEARING SHAFT .....	49
5. MEASUREMENT OF POWER AND THRUST.....	49

APPENDIX D. PART DRAWINGS.....	51
APPENDIX E. MANUFACTURING AND ASSEMBLY.....	62
APPENDIX F. COST ANALYSIS .....	62
APPENDIX G. DETERMINATION OF TARGET SPECIFICATIONS .....	66
APPENDIX H. ENGINE TACHOMETER SPECIFICATIONS.....	69
APPENDIX I. AMBIENT ENVIROMENTAL CONDITION SENSOR SPECIFICATIONS .....	71

**LIST OF FIGURES**

Figure 1 2010 Competition aircraft.....	1
Figure 2 O.S. MAX 0.61 engine .....	4
Figure 3 Side view of the compete assembly .....	7
Figure 4 Top view of the complete assembly .....	8
Figure 5 Front view of the complete assembly.....	9
Figure 6 Engine platform assembly.....	10
Figure 7 Engine platform assembly drawing .....	11
Figure 8 Frame body components .....	11
Figure 9 Frame body components drawing .....	12
Figure 10 Linear bearing system .....	12
Figure 11 Linear bearing system drawing.....	13
Figure 12 Mounted engine to pillow blocks. ....	14
Figure 13 Mounted engine to pillow blocks with deflection arm .....	14
Figure 14 Mounted engine to pillow blocks with platform and linear bearings .....	15
Figure 15 Streamline through a thin propeller disk with positive thrust .....	16
Figure 16 Thrust measuring sub assembly .....	18
Figure 17 The complete test stand .....	19
Figure 18 Universal engine mount adaptor plate.....	29
Figure 19 A-Type frame.....	29
Figure 20 First conceptual design .....	30

Figure 21 Second conceptual design .....	30
Figure 22 Third conceptual design.....	31
Figure 23 Fourth conceptual design .....	31
Figure 24 Fifth conceptual design.....	32
Figure 25 Sixth conceptual design model .....	32
Figure 26 Driveshaft torque sensor system .....	35
Figure 27 Torque sensor system.....	36
Figure 28 Friction Force .....	47
Figure 29 Bearing Load Test Setup .....	48
Figure 30 Side plate drawing .....	51
Figure 31 U-channel bracket drawing.....	52
Figure 32 Back plate drawing.....	53
Figure 33 Engine platform drawing .....	54
Figure 34 Engine mount drawing.....	55
Figure 35 Bearing shaft drawing .....	56
Figure 36 Torque arm drawing .....	57
Figure 37 Deflection arm drawing .....	58
Figure 38 Deflection arm mounting block drawing .....	59
Figure 39 Engine stop drawing .....	60
Figure 40 Fuel tank support drawing.....	61
Figure 41 Propeller thrust versus aircraft velocity .....	67
Figure 42 Schematic of the phototransistor based tachometer .....	69
Figure 43 Schematic of the weather sensor .....	71
Figure 44 Schematic of the weather sensor .....	72

**LIST OF TABLES**

TABLE I ENGINE TEST STAND NEEDS .....	3
TABLE II TARGET SPECIFICATIONS .....	5
TABLE III BILL OF MATERIALS .....	21
TABLE IV REQUIRED FASTENERS.....	22

TABLE V TEAM BRAINSTORMING.....	28
TABLE VI MDI TORQUE SENSOR SPECIFICATIONS .....	35
TABLE VII MDI LOAD SENSOR SPECIFICATIONS .....	36
TABLE VIII SIGNAL CONDITIONING SYSTEM SPECIFICATIONS .....	37
TABLE IX IOTECH 6222 DAQ SPECIFICATIONS .....	38
TABLE X GIRON MAGNETIC SHIELDING SPECIFICATIONS .....	39
TABLE XI METGLAS MAGNETIC SHIELDING SPECIFICATIONS .....	39
TABLE XII SIZING OF THE THRUST ROD .....	45
TABLE XIII SIZING OF THE BACK PLATE.....	46
TABLE XIV MANUFACTURING PROCESSES USED FOR VARIOUS TEST STAND COMPONENTS.....	62
TABLE XV DETAILED COST ANALYSIS.....	63
TABLE XVI UPDATED DETAILED COST ANALYSIS.....	64
TABLE XVII O.S. FX ENGINE SPECIFICATIONS .....	66
TABLE XVIII SPECIFICATIONS OF THE PHOTOTRANSISTOR TACHOMETER .....	70

## I. INTRODUCTION

Building model aircraft is a process referred to as aeromodelling and has been of interest to aerospace and aeronautical engineers throughout the history of aircraft. Aeromodelling provides the means to understand and predict the various factors influencing the performance of aircraft, which ultimately aids engineers in designing better working aircraft with enhanced characteristics. Moreover, by constructing models, one can understand the principles of flight and problems associated with construction. There exists a variety of aero models, which are classified according to their role and utility. They can be divided into two broad categories: static and dynamic. Powered radio-controlled (RC) aircraft are the most common types of dynamic models which fly with the aid of engines and propellers. This type of model is fitted with a radio receiver, mounted on the model, which receives the signal from the transmitter that is operated by the pilot. An example of a model air cargo plane is shown in Figure 1.



**Figure 1 2010 Competition aircraft**

The University of Manitoba Aero Design Team, consisting of mechanical engineering students, designs and builds RC aircraft for competition at annual Society of Automotive Engineers (SAE) Aero Design competitions. Competition flight scores are obtained by accumulating points, which are based on both the RC aircraft's performance and the team's

accuracy in predicting the performance of their design. Rigorous analysis is done by controlling and varying numerous design parameters in order to optimize the aircraft design and maximize the weight lifting capacity. Other calculations and verifications are performed to achieve high accuracy in predicting design performance. In order to accurately predict the performance of the aircraft, a full understanding of the performance characteristics of the engine is required. This is achievable by conducting several tests to obtain necessary information regarding the interaction of performance characteristics.

To date, the team has used the engine manufacturer's specifications in their calculations to predict the overall load carrying capability and performance of the aircraft. For a more successful performance in the annual competitions, the UMSAE Regular Class Aero Design Team would like to have in-house capabilities to test individual engines to obtain more accurate performance data and hence better predict overall aircraft performance.

### **A. PROJECT OBJECTIVES AND SCOPE**

The main purpose of this project is to design a test stand for a two-stroke model aircraft engine that is capable of measuring the key performance characteristics. These characteristics are thrust and torque as a function of wind speed and engine speed measured in revolutions per minute (rpm).

It is known that the performance of an aircraft engine is heavily dependent on the thrust it produces. Thrust is generated from the change in the momentum of the working fluid as a direct result of motion across the surface of the propeller. Torque results from the rotation of the propeller blades as a consequence of the engine power output. Any change in engine power output brings about a corresponding change in torque, which in turn affects the thrust and hence, the overall aircraft performance through the wind speed [1]. Therefore, all these ideas are interrelated and, in order to control and improve the performance, one needs to first determine how they interact.

Many considerations need to be taken into account in designing the test stand. These considerations are mainly defined by the client's needs which eventually determine the

project target specifications. Following a discussion with the client, a comprehensive list of the test stand characteristics was established and classified as presented in Table I [2].

**TABLE I  
ENGINE TEST STAND NEEDS [2]**

#	NEED
<b>I</b>	The Engine Test Stand Accommodates a 2 stroke RC model glow fuel engine.
a	The Engine Test Stand Accommodates electric RC aircraft engine.
b	The Engine Test Stand Accommodates a stock, unmodified engine.
c	The Engine Test Stand Allows for ease of removal or installation of engine under test.
d	The Engine Test Stand Accommodates a full range of propellers.
<b>II</b>	The Engine Test Stand Measures key engine performance data.
a	The Engine Test Stand Collects data autonomously
b	The Engine Test Stand Measures thrust and power simultaneously.
c	The Engine Test Stand Measures rotational speed.
d	The Engine Test Stand Measures the relative airspeed.
e	The Engine Test Stand Measures the ambient environmental conditions.
f	The Engine Test Stand Measures the fuel consumption.
g	The Engine Test Stand Minimizes influence on the test results.
<b>III</b>	The Engine Test Stand Emulates the operating environment
a	The Engine Test Stand Operates in a wide range of environments.
b	The Engine Test Stand Is operable in a moving environment.
c	The Engine Test Stand Minimizes environmental damage.
d	The Engine Test Stand Is robust.
<b>IV</b>	The Engine Test Stand Is portable.
a	The Engine Test Stand Can be disassembled and stored.
b	The Engine Test Stand Is lightweight.
c	The Engine Test Stand Accommodates a portable power source.
<b>V</b>	The Engine Test Stand Accommodates upgrades.
a	The Engine Test Stand Accommodates additional sensors.
<b>VI</b>	The Engine Test Stand Shall be easy to use

As shown in Table I, the first and one of the most important, considerations is the engine type. In designing an aircraft for competition, a major design constraint is the required engine. The rules state that regular class aircraft must use a single, unmodified O.S. FX 0.61 stock engine with an E-4010 muffler and must be fuelled by a 10% nitro methane mixture supplied at the competition [3]. Nevertheless, time and space permitting, the test stand should be capable of adapting to other engine types and sizes to be used by different teams [3]. The O.S. FX 0.61 MAX is shown in Figure 2.

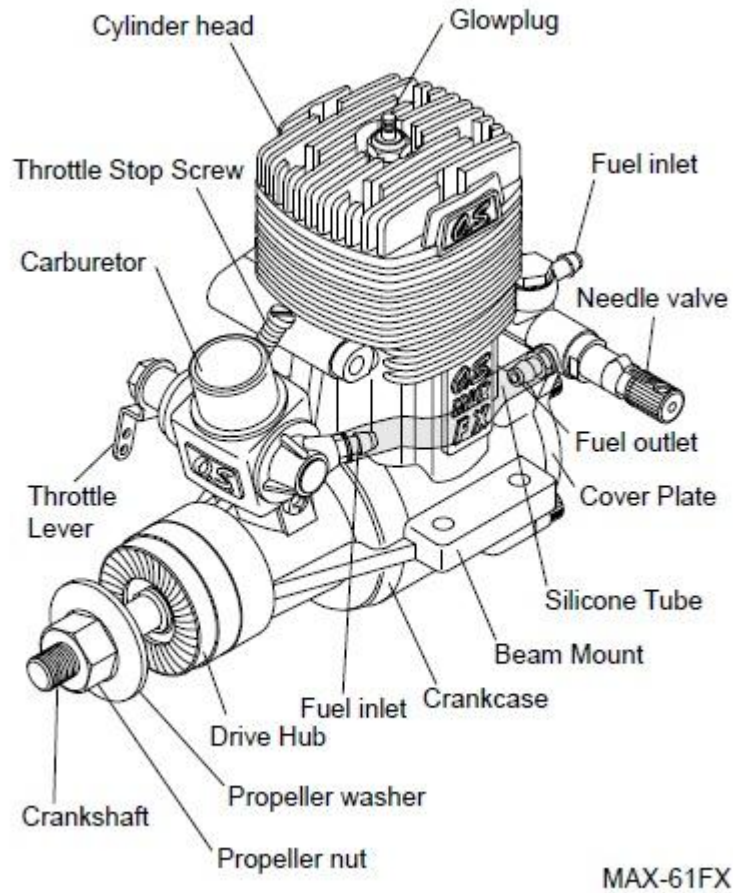


**Figure 2 O.S. MAX 0.61 engine[3]**

The test stand is to measure the thrust and torque simultaneously and collect, record, and analyze the data in an automated manner using electronic sensors. Thrust and torque are directly related to the wind speed and engine's rotational speed respectively. In order to obtain accurate and reliable measurements, the ambient conditions need to be identified so as to identify the environmental impacts on the test results.

The test stand is also required to be robust, portable, and operable in a dynamic environment. In order to meet these needs, the product including all of its subcomponents should be designed to be small in size and weight. Environmental protection is another aspect of the product. Noise, vibrations, emissions, and other destructive effects must be kept to minimum. For example, the engines exhaust contains a significant amount of oil residue which cannot be allowed to harm the electronic sensors of the test stand.

Finally, the test stand shall be versatile and able to accommodate future elements and upgrade. As the budget for the project is heavily dependent on sponsorship and external funding, the test stand components and additional features should be designed to be adapted sequentially as funding permits.

## B. TARGET SPECIFICATIONS

Once the customer needs were identified, the following technical specifications were developed. Table II lists the specifications including the marginal and ideal values with the corresponding unit of measure for each. These specifications were developed from the competition rules as set by the SAE rules committee and from the specifications for the engine.

**TABLE II**  
**TARGET SPECIFICATIONS [4][3]**

<b>Need</b>	<b>Metric</b>	<b>Marginal Specification</b>	<b>Ideal Specification</b>	<b>Unit of Measure</b>
<b>II-b</b>	Torque	0-10	N/A	<i>in * lbf</i>
<b>II-b</b>	Thrust	5-15	N/A	<i>lbf</i>
<b>II-c</b>	Rotational Speed	2000-17000	N/A	<i>RPM</i>
<b>I-e</b>	Propeller Diameter	11-14	N/A	<i>in</i>
<b>I-e</b>	Propeller Pitch	4-7	N/A	<i>in</i>
<b>II-d, III-b</b>	Airspeed	0-75	0-100	<i>ft/s</i>
<b>III-c</b>	Engine Noise	0-95	N/A	<i>dB</i>
<b>II-e, III-a</b>	Ambient Temperature	32-100	N/A	<i>°F</i>
<b>II-e, III-a</b>	Ambient Pressure	2100-3000	N/A	<i>lbf/ft<sup>2</sup></i>
<b>II-e, III-a</b>	Ambient Humidity	0-80%	N/A	<i>%</i>
<b>II-f</b>	Specific Fuel Consumption	0.3	N/A	<i>lbm/lbf * h</i>
<b>II-f</b>	Engine Temperature	70	N/A	<i>°F</i>
<b>IV-b</b>	Engine Test Stand Weight	30	N/A	<i>lbf</i>
<b>IV-c</b>	Power Source	12	110	<i>V</i>

The complete details as to how the system specifications were determined are presented in appendix G of this report.

## **II. DESIGN**

The final design of the test stand is presented here. The first section deals with the design features and will outline the unique and major features of the design. The component and assembly drawings are presented in the second section. The third section outlines the operation of the test stand. Finally, the overall cost and bill of materials are outlined in the fourth section. The underlying conceptual development phase will not be presented in detail in this report and a summary of the evolution of the design, as well as technical research can be found in appendices A and B.

### **A. FEATURES OF THE DESIGN**

The major components of the test stand include the engine mount, pivot shaft, torque arm, deflection arm, deflection limiters, platform, strain gages, bearings, and several supporting plates. Each of these components exhibit distinctive features which play a significant role in meeting the client's needs. This section aims to illustrate how these special features meet the objectives of the design.

The primary purpose of the design is to measure the key engine characteristics namely thrust and torque. This is accomplished by using the conventional strain gage based contact method. The use of strain gages allow for an automated and cost effective measuring system where all readings can be logged into a computer. Thrust will be measured using two strain gauges mounted to a tethering rod, which is sized to ensure that the engine mounting platform can be mounted to the linear guide. The rod will be threaded into the engine mounting platform and as the engine moves forward, the rod will stretch producing strain. Similarly, the torque will be measured using another set of strain gages mounted on the top and bottom of the deflection arm which is designed to sense the deflection produced by the torque arm as a result of engine's rotation. In both cases, the strains generated will be measured by a data acquisition system which measures the change in voltage. This change in voltage is related to the change in resistance produced as the wire in the gauges stretches. This provides a quantitative measure of thrust and torque

produced by the propeller. Figure 3 shows locations of the thrust shaft and torque deflection arm as well as the complete assembly.

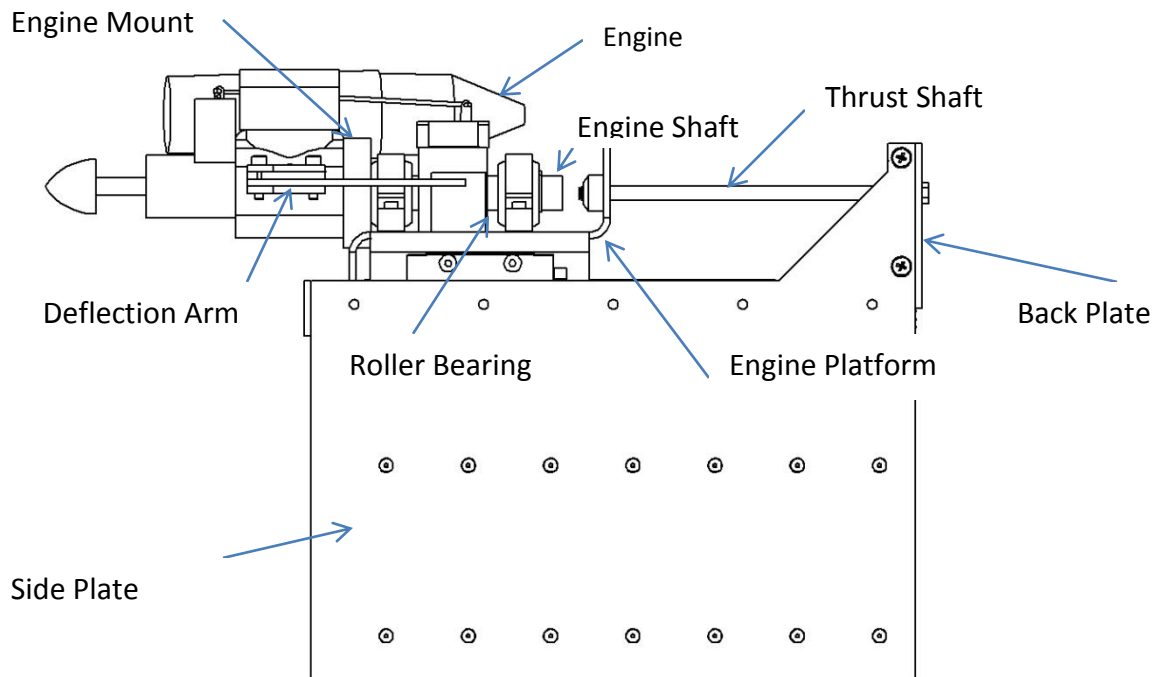


**Figure 3 Side view of the complete assembly**

In measuring torque and thrust simultaneously, the design must ensure measurement mechanisms do not interfere with one another. For this purpose, a shaft supported by two pillow block bearings is used. The shaft can freely rotate therefore allowing the engine to freely rotate, thus allowing measurement of torque. In addition, a linear bearing, outer frame and tethering rod constrain the motion of the engine in an axial direction. This ensures that the system will only measure the engine thrust output with negligible interference from engine twist and vibration. The configuration decouples the thrust and torque reactions generated by the engine, allowing separate measurements to be taken for each. The decoupling mechanism ensures independent and consistent measurements which is one of the major objectives of the design. These mechanisms are shown in Figure 4.

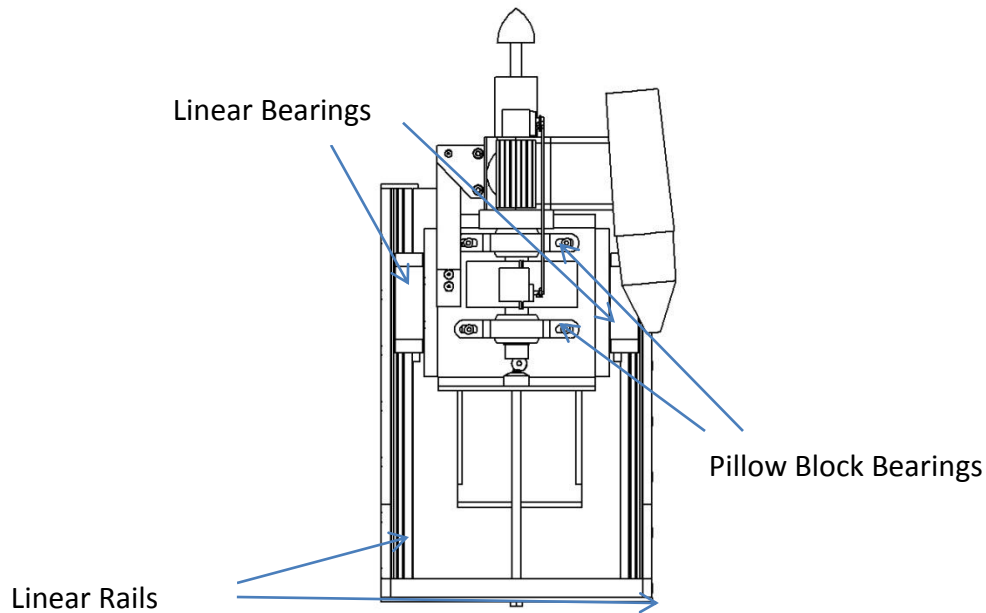


**Figure 4 Top view of the complete assembly**

Safety and robustness are additional significant design aspects that need to be addressed. The frame is designed to fully support the weight of the engine torque-measuring component and the engine itself, such that these components will be balanced. The linear guide will be fastened with countersunk hex bolts to the side plates which will be braced by two U-channels which keep the side plates in parallel and aligned. The size of the bracings and the thickness of the plates were designed to ensure that the linear guides do not fall out of alignment due to the weight and vibrations applied by the engine during operation. The rear plate is fastened to the side plates with two bracing supports extending from the side walls. This rear plate is designed to ensure that it will remain rigid when the axial rod is undergoing tensile loads. The platform is designed to provide a rigid base for mounting of all of the test stand components. These components are illustrated in Figure 5.

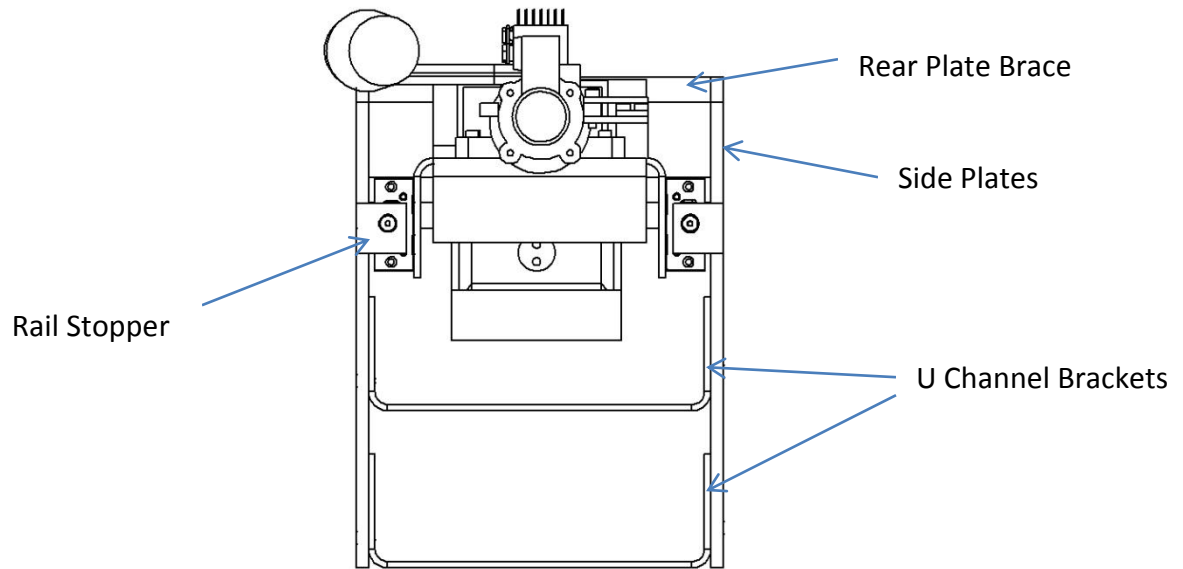


**Figure 5 Front view of the complete assembly**

The deflection limiter prevents overloading of the deflection arm by providing a physical stop for each deflection direction. This component is a pin, which is installed through the bearing shaft. A slot is cut out on the engine platform providing physical stops for the pin movement. When the engine is started, the torque applied is excessive, therefore the pin must also prevent excessive strain in the deflection arm. In the unlikely event that the torque arm and deflection arm decouple, they also provide a secondary stop to prevent engine rotation about the pivot axis.

The design becomes more attractive due to its unique features of adaptability and portability. The test stand consists of two separate pieces: the front and the back. The front portion is the torque-measuring system and the back portion is the thrust-measuring system. The two systems are separated by a supporting plate at the middle of the test stand. The complete frame of the thrust-measuring system is affixed to a frame and is attached to the torque-measuring system. The two-piece design allows the mounting plate to be interchangeable for mounting of different engine types and also simplifies the manufacturing process, reducing cost. The pivot shaft is machined from a bolt utilizing part of the rolled threads and head to secure the mounting plate. The side plates have an extended length to allow the use of a wide range of propellers. The extended length also

provides the space required to mount the fuel tank beneath the engine plate. The complete test stand, with overall dimensions of 11in x 7in x 9in and an estimated weight of 25lbs, is considered to be easily portable. Some of the components can be fabricated from even lighter materials which would further improve portability. The complete details of the technical aspects of the design can be found in appendix C.

## **B. PRODUCTION AND ASSEMBLY DRAWINGS**

Figure 6, shows the engine platform assembly, which consists of the engine platform, the deflection arm, the pillow block, and the bearing shaft. The engine is shown as transparent to illustrate how the assembly interfaces with the engine. Figure 7 presents an assembly drawing of the engine platform assembly.



**Figure 6 Engine platform assembly**

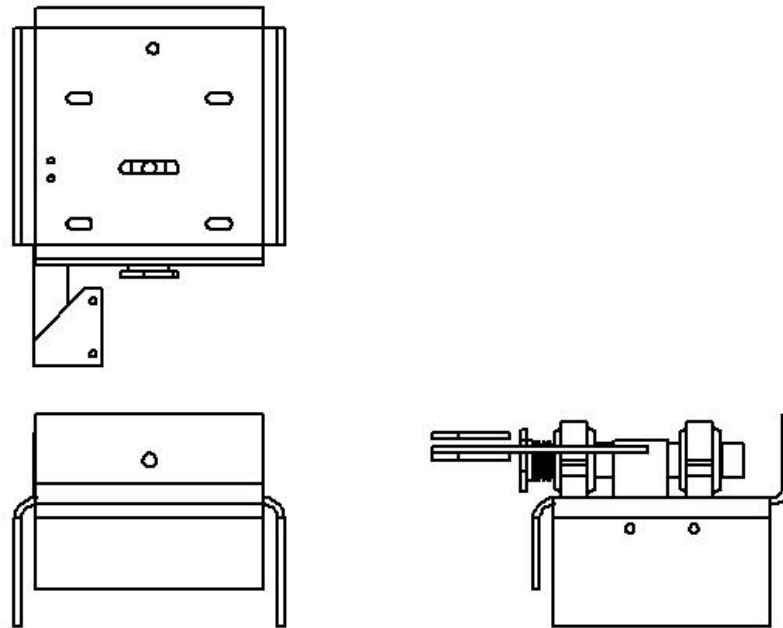


**Figure 7 Engine platform assembly drawing**

Figure 8 shows the frame body components. The side plates, back plate, U-brackets, and back braces comprise the body, along with the thrust shaft. The image also shows the engine, and engine platform assembly, as transparent, to demonstrate the relationship between them and the frame components. A drawing of the frame body components is shown in Figure 9.

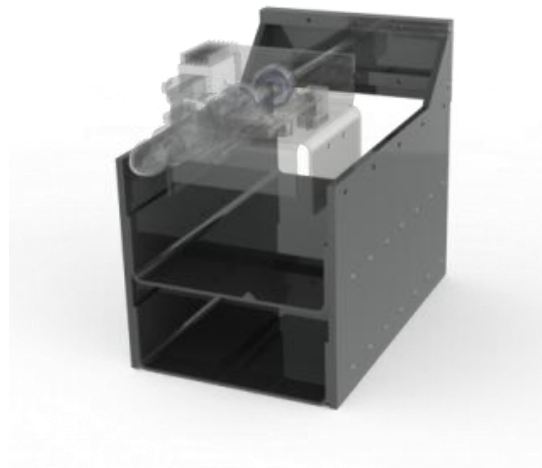


**Figure 8 Frame body components**

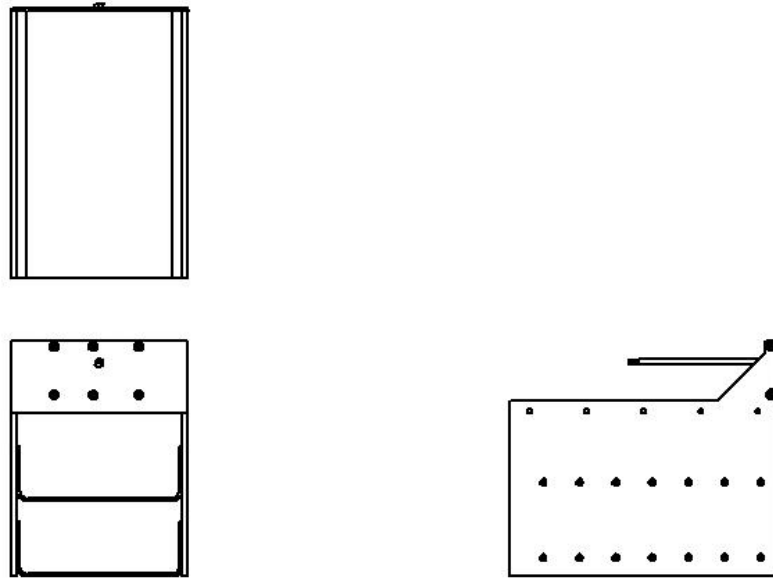


**Figure 9 Frame body components drawing**

The linear bearing system, which consists of a linear bearing which slides along a rail, is shown in Figure 10. The side wall that the rail attaches to is also shown. It is transparent to demonstrate how the linear bearing system attaches to the wall. A drawing of the linear bearing system is provided in Figure 11.



**Figure 10 Linear bearing system**

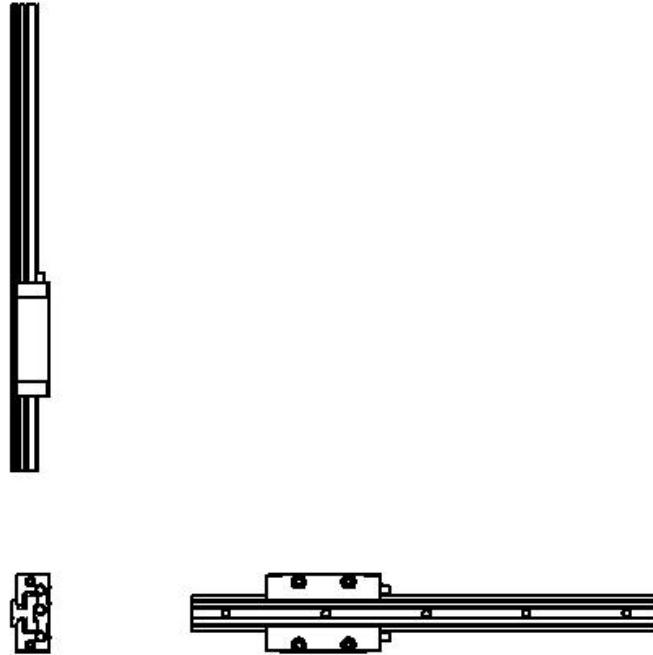


**Figure 11 Linear bearing system drawing**

Full detailed drawings of all components of the design, can be found in appendix D.

### **C. TEST STAND OPERATION**

The engine test stand consists of several key components which must work together to accomplish the task of characterizing the overall performance. The characteristics that are required to be measured are the thrust, rotational speed, torque, engine temperature, relative airspeed, the fuel consumption, and the ambient environmental conditions. First the engine and associated propeller must be mounted to the engine mount which is attached to a shaft which is resting in a set of pillow block roller bearings. This sub assembly is shown in Figure 12.

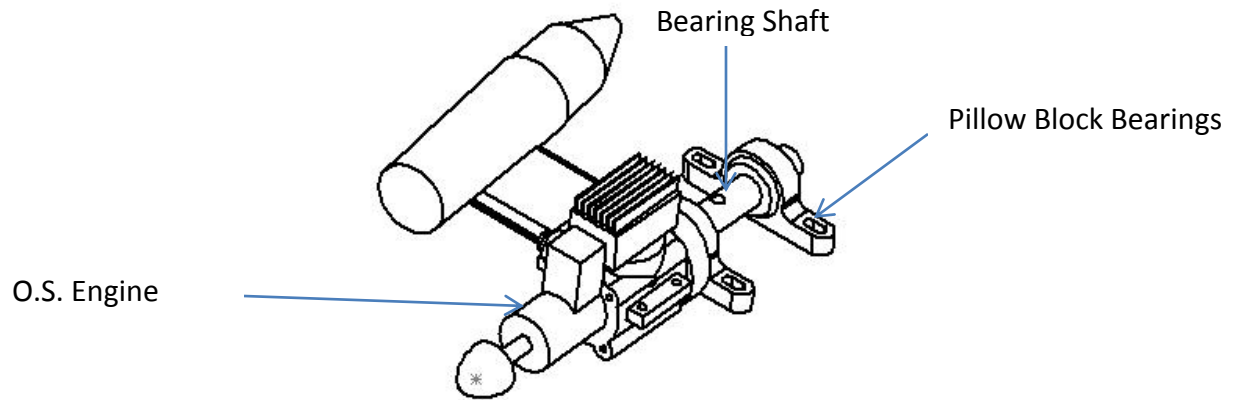


**Figure 12 Mounted engine to pillow blocks.**

When mounted through the pillow blocks as shown in Figure 12, the engine will rotate freely in reaction to the rotation of the propeller. Therefore to ensure that the engine will not rotate, and to measure the torque generated by the propeller, an arm is extended from the side mounts of the engine, which meets a beam with strain gages attached. As the engine attempts to rotate, the beam will deflect. The resulting strain will be measured and therefore the torque, which is a function of force over a distance, can be determined. This assembly is shown in Figure 13.

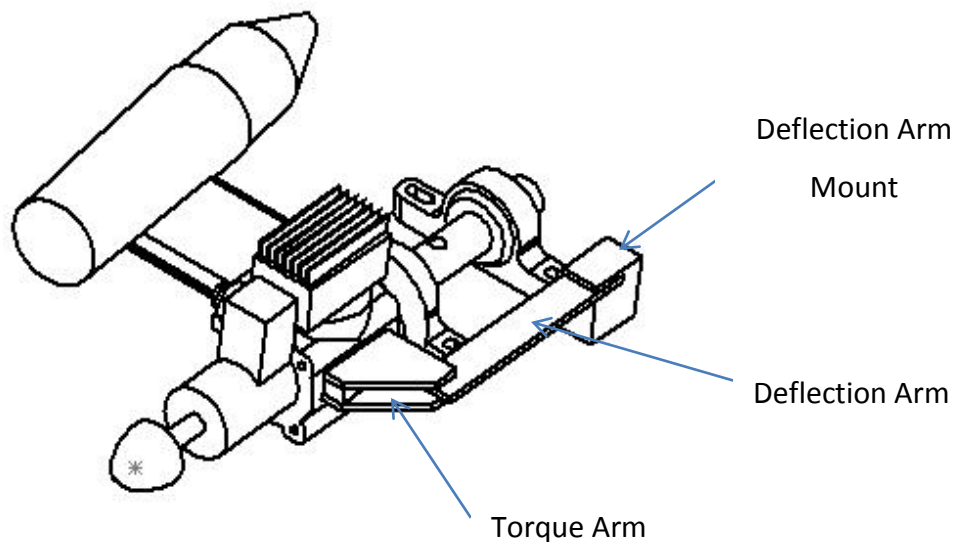


**Figure 13 Mounted engine to pillow blocks with deflection arm**

This entire construct is then mounted to a platform as shown in Figure 14 which is attached to a pair of linear bearings. This completed torque sensing system is shown in Figure 14.

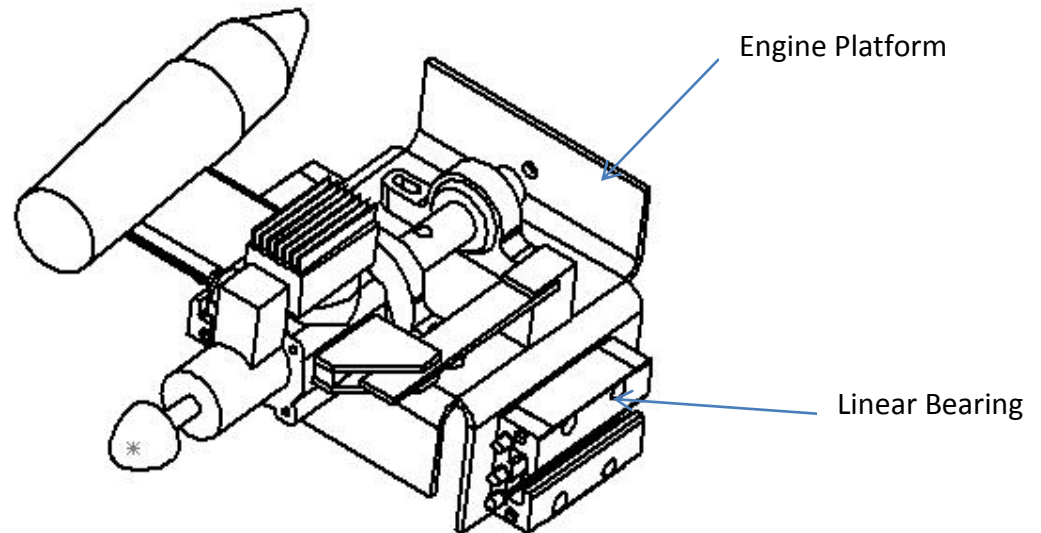


**Figure 14 Mounted engine to pillow blocks with platform and linear bearings**

As shown in Figure 14, the engine will rotate freely without the presence of the deflection arm and the platform will be rigid enough to support the engine without flexing. The deflection arm will bend in response to the rotation of the engine, and strain gages mounted on the beam will measure the strain. This strain will then be converted into a force which, when multiplied by the distance from the engine center will represent the overall torque. The strain gages will be connected to an IOtech 6224 data acquisition system, which can compensate for vibrations and other anomalous behaviour, which will increase the accuracy of the results.

This subassembly will combine with an optical tachometer which will measure the rotation speed of the propeller in revolutions per minute. This will be done with a non-contact tachometer which will consist of either a phototransistor or proximity sensor. Essentially the system senses the propeller passing in front of the sensor and keeps count of the number of pulses per minute and presents this as the number of rotations per minute. This

sensor would be mounted to the platform behind the engine or conversely attached to the side plate. A full specification of a system can be found in appendix H.

Finally to control the engine throttle and fuel/air mixture, two servo motors are mounted to the platform as well. These motors are controlled by the test software remotely, and adjust the engine as necessary to allow for a full range of propeller rpm. Furthermore, through software, the optimal setting for maximum power and thrust are found by setting up a test pattern.

Thrust is produced from the propeller converting the rotational motion into translational motion, essentially acting like a screw being driven forward with every rotation. Propellers can generate positive and negative thrust, but for the purposes of this report the assumption is that the propeller will be generating positive thrust only. Since the aircraft, for the purposes of the Aero Design competition, is operating at a Mach number below 0.3, the air will be considered to be in the incompressible regime and therefore momentum theory will be applied. For the purposes of this theory, the propeller is replaced by a thin disk with an infinite number of blades. Figure 15 shows the air flow which is responsible for the generation of thrust [1].

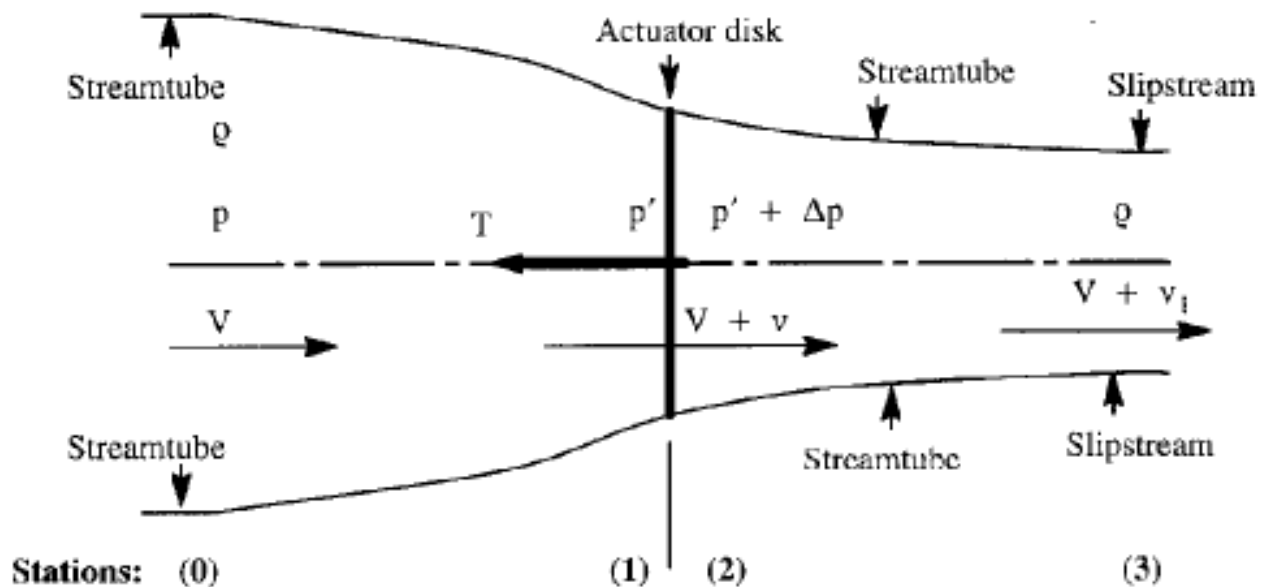


Figure 15 Streamline through a thin propeller disk with positive thrust[1]

Station 0 represents the conditions ahead of the aircraft, where  $V$  represents the velocity of the ambient air, and  $P$  represents the air pressure. Immediately after the propeller disk, the rotational energy is added to the air stream in the form of an additional velocity,  $v$ , and to properly balance the flow, additional pressure is also added to the airstream. Applying Bernoulli's equation and the principles of linear momentum to the system yields the following relationship shown in the Equation (1) below [1].

$$T = A\rho(V + v)v_1 \quad (1)$$

As a consequence of ensuring that momentum is conserved as the aircraft velocity increases, the added velocity component decreases and therefore the thrust decreases [1]. Thus a thrust measuring system will be designed, as part of the engine test stand, to operate in a moving frame to measure the decrease in thrust. The primary rationale for this need is to accurately measure the change in thrust during a take-off ground roll, due to the client need for an accurate measurement of the lifting capacity of the aircraft for the purposes of the competition.

For the purposes of this simulation, a linear bearing, outer frame and tethering rod constrain the motion of the engine in an axial direction. This ensures that the system will only measure the engine thrust output with negligible interference from engine twist and vibration. The frame is designed to fully support the weight of the engine torque measuring component and the engine itself, such that these components will be balanced. The linear bearings are NSK LH high load capacity precision linear guides and bearings. The roller bearings will allow the engine to slide freely with minimal friction.

The thrust will be measured using strain gauges which will be mounted as on a rod composed of aluminum 7075-T6 which is sized to ensure that the engine mounting platform can be mounted to the linear guide. The rod will be threaded into the engine mounting platform and as the engine moves forward, the rod will stretch producing strain. This strain will be measured by an IOtech 6224 module which measures the change in voltage. This change in voltage is related to the change in resistance as the wire in the gauge stretches. The strain is converted to stress, and since the area of the rod is fixed the force acting on

the rod can be calculated. This force is the thrust produced by the propeller. The full subassembly which consists of the linear rails, the frame and the tether are shown in Figure 16.

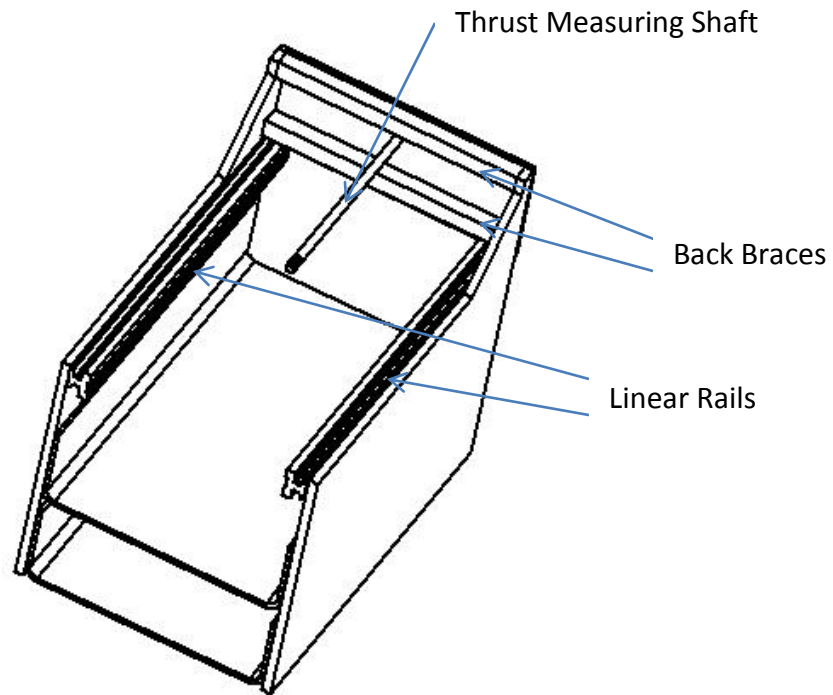


**Figure 16 Thrust measuring sub assembly**

The free end of the rod mounted to the rear shaft is then fastened to the torque subassembly and the system is completed. This completed system is presented in Figure 17.

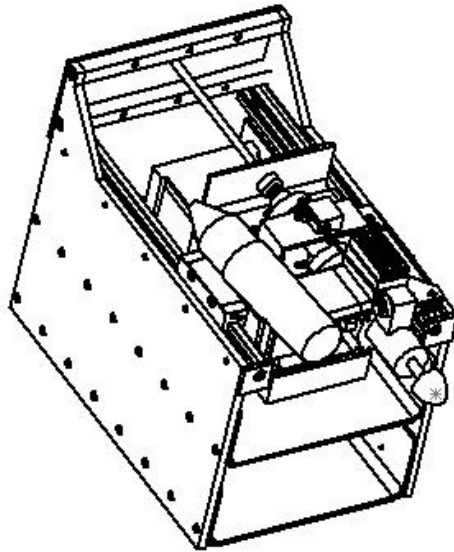


**Figure 17 The complete test stand**

The IOtech 6222 will also be used along with a thermocouple to measure the engine operating temperature. The two DAQs will be mounted in the lower shelf of the stand. A second thermocouple will be used to measure the ambient temperature conditions. Since the ambient conditions are relatively constant or change slowly, the pressure will be measured using an external barometer and recorded manually. Finally a pitot tube will be mounted in front of the stand to measure the forward air speed. The full set of technical details on the ambient condition sensor is outlined in appendix I.

To simulate a take-off ground roll, the stand can be mounted to a moving object which is accelerated slowly up to take off speed while measuring results. The data will be stored within a computer and plots of torque and power versus revolutions per minute and thrust versus forward air speed can be generated.

#### **D. OVERALL COST AND BILL OF MATERIALS**

Since this design will be implemented by a student group, with very limited funding, maintaining a low cost is of high importance. In order to achieve a high quality design which met all of the needs and requirements as specified by the client, while minimizing the project costs, care was taken in selecting materials and component suppliers. A number of

components, such as strain gauges and load cells, are property of the University of Manitoba, and available to the Aero Design Team to use free of charge. Other items, for example the fuel tank, belong to the Aero Team and can be used in this design. Such availabilities were key deciding factors for a number of design choices made. The total cost of the design, when taking into account the market values for all required materials, parts, and services, is \$4,896.00. The total raw material cost is estimated as \$580.30, and the total machining cost as \$1,130.00. The entire cost break down, which outlines the detailed costs of each component, is presented in Appendix D.

The Aero Team typically has access to offcut aluminum from a local company, and has in the past received donated steel from Brunswick Steel. The team also has access to a number of machinists at the University, who are willing to donate their time to machine parts for the student organization. After taking into account anticipated sponsorship and in-kind donations, the total cost of this project is estimated as \$240.00. This cost is substantially lower than the total design cost, and as a result, much more affordable for a team with such a small budget.

The detailed bill of materials for this project is provided in TABLE III. The bill of materials lists all components of the design by the description of their role in the engine test stand and their part numbers. For components that would be purchased in their entirety, requiring no manufacturing, the manufacturer's part numbers are used. For the other parts, most of which are machined, part numbers were assigned. The required part quantities are listed, along with the part or material vendor. The material of the component is given, and the form of material, and the required material size, is also listed.

**TABLE III  
BILL OF MATERIALS**

<b>Item</b>	<b>Description</b>	<b>Part Number</b>	<b>QTY</b>	<b>Vendor</b>	<b>Material</b>	<b>Form</b>	<b>Specifications</b>
1	Back Brace	E10-P006	2	Brunswick Steel	Steel	Bar	7[in] x 0.5[in] x 0.5[in]
2	Back Plate	E10-P005	1	Brunswick Steel	Steel	Sheet	9[in] x 3[in] x 0.125[in]
3	Bearing Shaft	E10-P0011	1	Brunswick Steel	Stainless Steel	Machined Bolt	7/8-9 x 3.75[in]
4	Deflection Arm	E10-P0016	1	Brunswick Steel	Steel	Sheet	4[in] x 1[in] x 0.125[in]
5	Deflection Arm Mounting Block	E10-P0017	1	Brunswick Steel	Steel	Bar	1[in] x 0.75[in] x 0.625[in]
6	Engine Mount	E10-P0010	1	Resistaloy	Aluminum	Plate	2 [in]
7	Engine Platform	E10-P007	1	Brunswick Steel	Steel	Sheet	9[in] x 8[in] x 0.125[in]
8	Engine Stop	E10-P0023	2	Brunswick Steel	Steel	Sheet	1[in] x 1[in] x 0.125[in]
9	Fuel Tank	DUB424	1	Dubro	Plastic	N/A	7.5[in] x 3.06[in] x 2.5[in]
10	Fuel Tank Support	E10-P0026	1	Cellar Dweller	Balsa	Sheet	25[in] x 4[in]
11	Limiter Pin	E10-P0024	1	Brunswick Steel	Steel	Rod	2.25[in] x 0.5[in]
12	Linear Bearing	E10-A003	2	NSK	N/A	N/A	N/A
13	Load Cell	MLP-10	1	Transducer Techniques	N/A	N/A	N/A
14	Pillow Block Bearing	KSTI-10	2	Igubal	N/A	N/A	N/A
15	Retaining Ring	1460-75	1	ARCON	Steel	Wire	0.78 [in]
16	Side Plate	E10-P001	2	Brunswick Steel	Steel	Sheet	14i[in] x 10[in] x 0.25i[in]
17	Throttle Linkage	E10-P0029	1	Cellar Dweller	Steel	Push Rod	5[in] x 0.1[in]
18	Throttle Servo	S185	1	Futaba	N/A	N/A	N/A
19	Servo Arm	E10-P0031	1	Futaba	N/A	N/A	N/A
20	Throttle Servo Mount	E10-P0032	1	Resistaloy	Aluminum	Sheet	7[in] x 1.25[in] x 0.25[in]
21	Thrust Shaft	E10-P0014	1	Resistaloy	Aluminum	Rod	7[in] x 0.5[in]
22	Thrust Strain Gauge	CEA-13-240UZ-120	2	Vishay	N/A	N/A	N/A
23	Torque Arm	E10-P0015	2	Brunswick Steel	Steel	Sheet	1.5[in] x 1.5[in] x 0.125[in]
24	Torque Strain Gauge	CEA-13-240UZ-120	2	Vishay	N/A	N/A	N/A
25	U-Bracket	E10-P004	2	Brunswick Steel	Steel	Sheet	14[in]x11[in]x 0.125[in]

The bill of materials does not include the fasteners necessary for this design. A detailed list of the fasteners required is provided in TABLE IV. The part description outlines how each fastener will be used within the test stand assembly. The fastener quantity and material required are listed, and the type of fastener is noted. The specifications of each fastener are also provided. The total cost of fasteners was estimated to be \$25.00, at bulk hardware costs.

**TABLE IV  
REQUIRED FASTENERS**

<b>Item</b>	<b>Part Description</b>	<b>QTY</b>	<b>Material</b>	<b>Type</b>	<b>Specifications</b>
<b>1</b>	Back Brace to Back Plate Attachment Bolts	6	Steel	Socket FCHS	B18.3.5M - 4 x 0.7 x 16-16N
<b>2</b>	Back Brace to Side Plate Attachment Bolts	4	Steel	Type I Cross Recessed FHMS	B18.6.7M - M4 x 0.7 x 8-8N
<b>3</b>	Deflection Arm Mounting Bolts	2	Steel	SCHC Screw	0.112-48x1.125x1.125-HX-N
<b>4</b>	Engine Stops to Rail Attachment Bolts	2	Steel	Socket FCHS	B18.3.5M - 4 x 0.7 x 8-8N
<b>5</b>	Linear Bearing to Engine Platform Attachment Bolts	4	Steel	Countersunk Hex Bolt	M4x24
<b>6</b>	Linear Rail to Side Wall Attachment Bolts	10	Steel	Countersunk Hex Bolt	M5x20
<b>7</b>	Load Cell to Fuel Tank Support Attachment Bolts	2	Steel	SCHC Screw	0.19-32x0.25x0.25-HX-N
<b>8</b>	Pillow Blocks to Engine Platform Attachment Bolts	4	Steel	Countersunk Hex Bolt	M5x20
<b>9</b>	Thrust Shaft Nut	1	Steel	Hex Nut	0.25-20UNC
<b>10</b>	Torque Arm Machined Screw	2	Steel	SCHC Screw	0.086-64x0.3125x0.3125-HX-N
<b>11</b>	Torque Arm Sockethead Cap Screw	2	Steel	Hex SHCS	B18.3.1M - 4 x 0.7 x 16-16NHX
<b>12</b>	U-Bracket to Side Plate Attachment Bolts	30	Steel	SCHC Screw	0.112-48x0.375x0.375-HX-N

The above bill of materials and cost analysis is detailed in Appendix F following this report.

### III. CONCLUSIONS

The engine test stand design satisfies the Aero Team's requirements. It accommodates the OS FX 0.61 engine currently used by the Regular Class Aero Team, and requires no engine modifications in order to perform testing. The test stand accepts a rear mount configuration common to engines used at the Aero Design Competition. This allows the accommodation of other engines by replacing the mounting plate, - a relatively inexpensive component which can be manufactured by the Aero Team. The test stand is also able to operate with a full range of propellers by having no components cross the propeller plane.

The key performance data of thrust and torque are measured simultaneously by the test stand and collected using an existing data acquisition system. The stand also measures engine rpm, and ambient temperature with the capability of measuring airspeed. However barometric pressure will need to be recorded separately before tests.

To minimize the test stand's influence on the test results, its channel shape frame supports the test equipment while having a low frontal surface area. Moreover, it is robustly constructed from heavy plate which will keep vibration transmission low, reducing measurement disturbance. The decoupling of torque and thrust also eliminates potential interference of measurements. In addition, the mounting of the fuel tank to the engine platform prevents the measurement of forces transmitted through the fuel lines.

At around 25 lbs, the test stand is portable and can take measurements independently. Strap points allow dynamic testing on the outside of a moving vehicle or to secure the stand to a table for static measurements. Electrical power can be supplied from a car battery when needed by using an inverter. When testing is completed, the measurement equipment can be removed for safe storage leaving only the main frame which does not take up much space.

In conclusion, the design is simple and safe to operate not requiring near operators and incorporates various safety features such as stops for ensuring component restraint. The system is low cost, lightweight and easily stored. This system also meets all of the

necessary client requirements therefore the design is sound. Therefore it is the recommendation of the design team that the University of Manitoba Aero Design Team should begin construction of this system once it has been formally approved.

## IV. REFERENCES

- [1] J. Roskam and C.-T. E. Lan, *Airplane Aerodynamics and Performance*. Lawrence, KS: DARcorporation 1997.
- [2] P. Labossiere, (private communication), Sept. 14, 2010.
- [3] SAE Rules Committee. (2011, Sept.). 2011 *Collegiate Design Series: Aero Design® East and West Rules* [Online]. Available: <http://students.sae.org/competitions/aerodesign/rules/rules.pdf> [Sept. 15, 2010].
- [4] O.S.® Engines Mfg. Co., LTD. (2001). *O.S. ENGINES MAX-50SX RING & 40, 46, 61, 91 'FX SERIES': OWNER'S INSTRUCTION MANUAL* [Online]. Available: [http://www.osengines.co.jp/english/line\\_up/engine/air/aircraft/manual/50sx\\_40-91fx.pdf](http://www.osengines.co.jp/english/line_up/engine/air/aircraft/manual/50sx_40-91fx.pdf) [Oct.2, 2010].
- [5] S. Bitar, J. S. Probst and I. J. Garshelis. (2000). *Development of a Magnetoelastic Torque Sensor for Formula 1 and CHAMP Car Racing Applications*. SAE International, Detroit, MI [Online]. Available: <http://www.magcanica.com/files/SAE2000.pdf> [Nov 01, 2010].
- [6] I. J. Garshelis. (2000) *Torque and power measurement*. [Online]. Available: CRCnetBASE [Oct. 22, 2010].
- [7] Magneto-Elastic. (2010) *Magneto-Elastic/Method* [Online]. Available: <http://www.methode.com/sensors-and-switches/torque-sensing/magneto-elastic.html> [Nov 01,2010].
- [8] Allegro MicroSystems. (2010) *Hall-Effect Sensor ICs* [Online]. Available: <http://www.allegromicro.com/en/Products/Categories/Sensors/index.asp> [Nov 01, 2010].

- [9] Allegro Microsystems. (2010) *Allegro Microsystems Inc, Home Page* [Online]. Available: <http://prostores2.carrierzone.com/servlet/AllegroMicroSystems/StoreFront> [Nov 01, 2010].
- [10] MagCanica Inc. (2010) *MagCanica Inc :: Products* [Online]. Available: <http://www.magcanica.com/products.html> [Nov 01, 2010]
- [11] National Instruments. (2010) *NI9211 0 4-Channel, 14 S/s, 24-bit, +/- 80 mV, Thermocouple Input Module – National Instruments* [Online]. Available: <http://sine.ni.com/nips/cds/view/p/lang/en/nid/208787#specifications> [Nov 01, 2010].
- [12] IOtech. (Nov 02, 2009) *New 6000 Series DAQ Modules for Temperature and Voltage* [Online]. Available: [http://www.mccdaq.com/press\\_releases/pr\\_6222\\_6230.pdf](http://www.mccdaq.com/press_releases/pr_6222_6230.pdf) [Nov 01, 2010]
- [13] The EMF Safety Superstore. (2010) *Magnetic Field Shielding Materials* [Online]. Available: <http://www.lessemf.com/mag-shld.html> [Nov 01, 2010].
- [14] Roymech. (Oct 09, 2010) *Coefficients of Friction* [Online]. Available: [http://www.roymech.co.uk/Useful\\_Tables/Tribology/co\\_of\\_frict.htm](http://www.roymech.co.uk/Useful_Tables/Tribology/co_of_frict.htm) [Nov 01, 2010].
- [15] Roymech. (June 06, 2010) *Roller Bearing Friction* [Online]. Available: [http://www.roymech.co.uk/Useful\\_Tables/Tribology/Bearing%20Friction.html](http://www.roymech.co.uk/Useful_Tables/Tribology/Bearing%20Friction.html) [Nov 01, 2010].
- [16] J. Ilott and A. Oldenkamp, *Design of a Heavy-Lift Radio-Controlled Aircraft*. Winnipeg, MB: University of Manitoba 2009.
- [17] STEFANV.COM. (Jul 19, 2010) *Build an LED Bargraph Optical Tachometer* [Online]. Available: <http://www.stefanv.com/electronics/tachometer.html> [Nov 01, 2010].

[18] Sparkfun Electronics, "USB Weather Board v2 Datasheet." Boulder, CO: Sparkfun, 2008.

## APPENDICES

### A. CONCEPT DEVELOPMENT

The conceptual development of the engine test stand was performed in stages. The first stage was brainstorming which was performed as a team exercise. Based on our individual experience and knowledge, the Aero Team came up with a list of ways in which the test stand could perform each function, which is outlined in our design objectives. The team began by separating the test stand into its general components, and then generated ideas for ways the function or feature of each of those components could be met. Table V outlines the results from this brainstorming session.

**TABLE V  
TEAM BRAINSTORMING**

Means Feature/ Function	1	2	3	4	5	6
<b>Sense Force</b>	Load-cell	Electro-magnet	Strain Gage	Spring/Deflection	Gravity Force Balance	----
<b>Sense Torque</b>	Electromagnet	Eddy current Transducer	Electric Motor	Torque Load cell	Arm and Strain Gage	Shaft Twist
<b>Sense Engine rpm</b>	Hall Effect Sensor	Proximity sensor	Optical sensor	----	----	----
<b>Sense Air Speed</b>	Pitotube	Anemometer	Micro-manometer	----	----	----
<b>Sense Temperature</b>	Thermocouple	Thermometer	Infrared gun	----	----	----
<b>Sense Fuel Consumption</b>	Change in weight	Fuel Flow Sensor	----	----	----	----
<b>Power Source</b>	Battery	Wall Outlet	Car Outlet	Solar Panel	Fuel Cell	----
<b>Engine Mounting</b>	Bolted Engine specific Plate	Clamp	Universal Mounting Plate	Straps	Tether	Glue

A series of concepts were generated and examined further through external searches and research. The concept selection process was broken down into sensors, power source, frame and engine mount. For the sensors the debate was between contact and non-contact sensor systems. Hull effect sensors were considered as a potential sensor system to measure thrust and torque. This research is presented in Section 1. Screening the potential

power sources led to the selection of an external source, such as a battery or electric outlet. Screening the engine mounts led to the selection of a universal engine mount which is shown in Figure 18. The A-type frame was selected through the screening process and is shown in Figure 19.

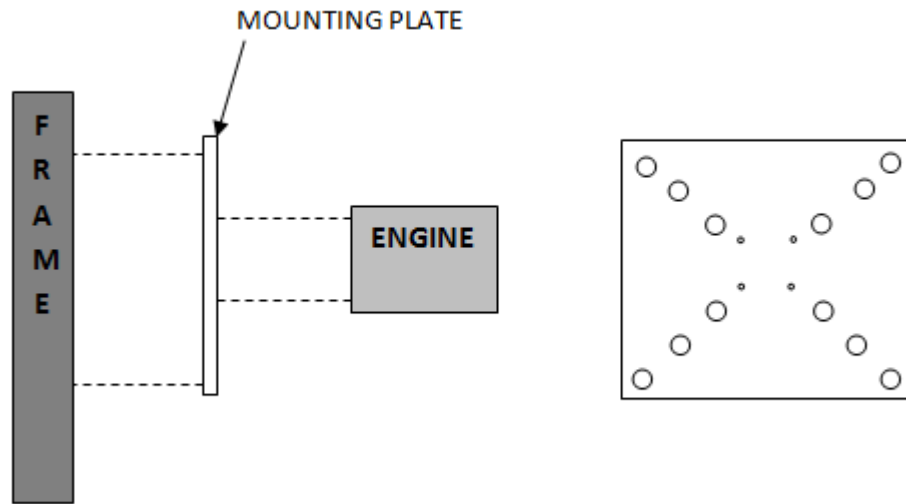


**Figure 18 Universal engine mount adaptor plate**

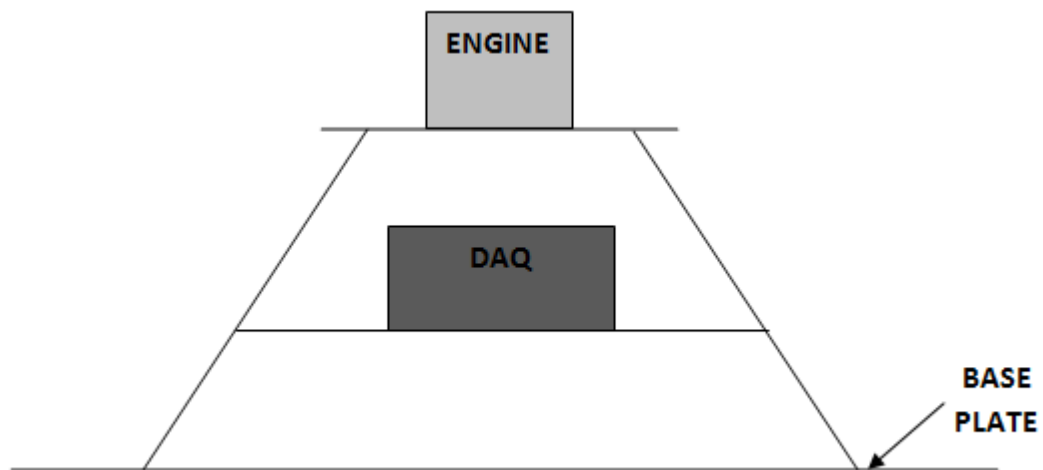


**Figure 19 A-Type frame**

The final engine test stand also underwent a series of developments during the design phase. The evolution of the final model is presented in a series of figures below.

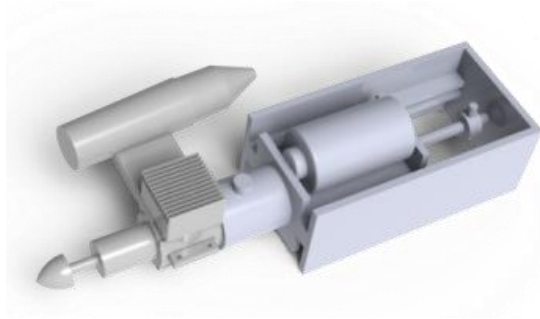


**Figure 20 First conceptual design**

The above concept in Figure 20 utilizes a torque load cell to measure the torque as well as a tension load cell to measure the thrust. The linear bearing is merely a channel groove and the stand is meant to be affixed to a larger frame for support. Due to a cost of 1000\$ for a torsion load cell, the team opted to eliminate that load cell from the design. This development leads to the second concept, which is presented in Figure 21.

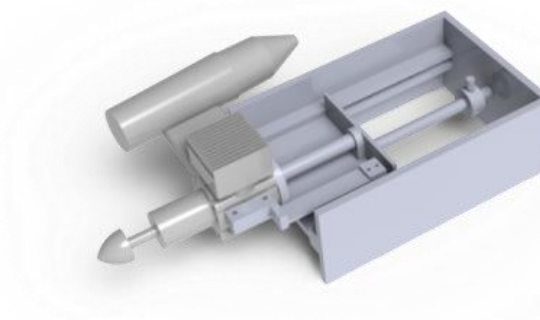


**Figure 21 Second conceptual design**

The second concept shown in Figure 21 replaces the torque load cell with a deflection arm. As the engine would twist due to the propeller, the arm would deflect, allowing for the measurement of torque through strain gages. The stand would still require a separate frame, which would be resolved in with the concept presented in Figure 22.



**Figure 22 Third conceptual design**

The third concept of the test stand adds two roller bearings supporting a shaft to which the engine is mounted. The system is now also a self-contained unit, which can be mounted on any surface with enough clearance so that the propeller will not strike the ground. The frame is made up of rigid steel, so the design is sturdy and durable. As well, the linear rail is now comprised of NSK linear bearings, which are sized for the application and loads. Further refinement of the design is shown in Figure 23.

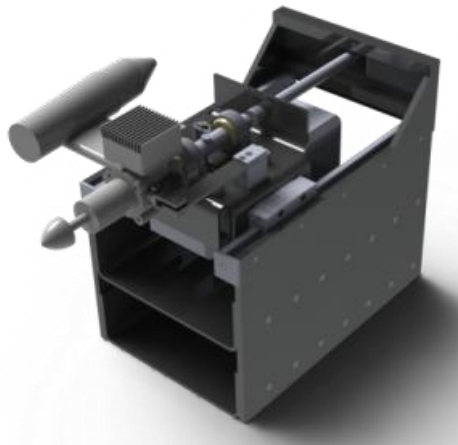


**Figure 23 Fourth conceptual design**

The fourth revision of the design adds IGUbal spherical bearings to support the engine shaft, and braces the back plate. This back plate holds the shaft to which strain gages are affixed for thrust measurement. Therefore the load cell which would measure the thrust is

no longer part of the design. As well the moment arm is now designed for a maximum deflection, using a pin mounted through the bearing shaft, which will hit two stops ensuring that the deflection arm will not exceed safe limits. The next stage of refinement is shown in Figure 24.

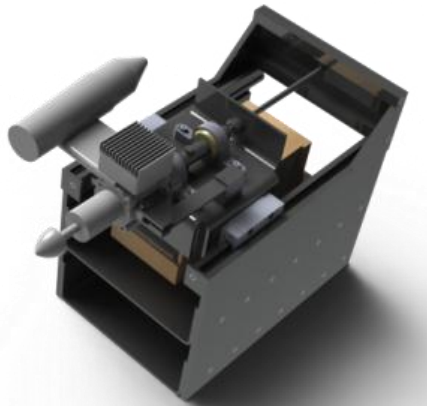


**Figure 24 Fifth conceptual design**

Figure 24 also shows the addition of the fuel tank carrier. The tank is suspended from the bottom of the engine platform and is attached to a load cell. This load cell will be used to measure the fuel consumption, by measuring the mass change over time within the tank. The final revision of the design is shown in Figure 25.

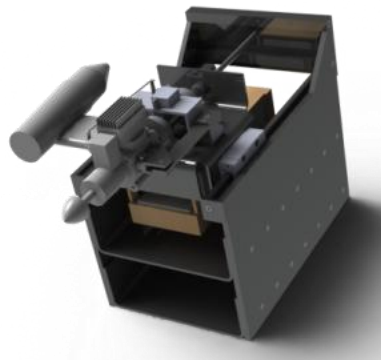


**Figure 25 Sixth conceptual design model**

Figure 25 shows the current revision as displayed in Section II of the report. This revision adds the engine throttle servo as well as the linkage cable connecting to the throttle control

on the engine. Other systems are not shown in the design, but will be incorporated as additional sensors. The data acquisition system will be placed in the lower shelf and a plate will be installed to protect it from the engine emissions.

In summary, this shows the development of the design from nascent stages to the finished design. The final design meets all customer needs and specifications and will perform the necessary tasks.

## **B. NON-CONTACT SENSORS**

Magnetoelastic torque and load sensors were considered as potential measuring devices to perform the necessary engine measurements. Magnetoelasticity refers to the influence of an applied elastic stress on the magnetic properties of a material [5]. A magnetoelastic material is, therefore, a material that experiences a change in magnetic properties under the action of an elastic stress. This change is detected and measured by means of Magnetoelastic sensors.

Magnetoelastic sensors offer numerous advantages. They measure engine performance properties without requiring a direct physical contact with the engine shaft. The sensors are compact, light, and exhibit low sensitivity to thermal conditions. Nevertheless, the reliability of measurements by such sensors is heavily determined by the environmental conditions. When using magnetoelastic sensors, the environment surrounding the sensors must be controlled carefully in order to avoid interference from ferromagnetic tools and components [5].

A magnetoelastic torque transducer captures the effect of stresses that transmit torque. The transmitted torque is measured by examining how the magnetic properties of the magnetoelastic material, mounted on the engine shaft, vary. The magnetoelastic material is the polarized bands shown in Figure 26. Upon the action of torsional stresses, the solid arrows, which indicate the direction of magnetization, are distorted. The green elements are the magnetoelastic sensors that detect this distortion and provide an output signal which allows measurement of the transmitted torque [6].

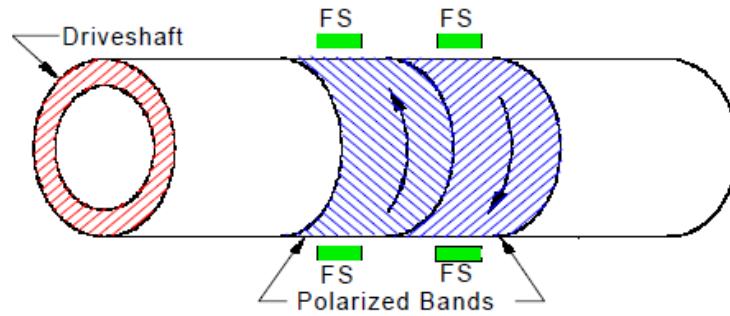


**Figure 26 Driveshaft torque sensor system [5]**

It is important to mention that if a magnetoelastic polarized-band approach is used, the engine shaft material must be ferromagnetic and must possess magnetoelastic properties [5].

MDI produces sensors which can measure the torque, both axially and radially. The general specifications for MDI torque sensors are provided in TABLE VI. The sensors can operate on any sized system, which can be operating at a wide variety of speeds [7].

**TABLE VI  
MDI TORQUE SENSOR SPECIFICATIONS [4]**

<b>Range</b>	<b>0 to +/- 1Nm to 0 to +/- 50 kNm</b>
<b>Resolution</b>	0.1 Nm to 0.5 Nm
<b>Accuracy</b>	0.5% to 1.0%
<b>Repeatability</b>	0.25% to 0.4%
<b>Response to Change</b>	1kHz to 20kHz
<b>Substrate</b>	6.0mm to 600mm
<b>Operating Temperature</b>	-40C to 180C
<b>Power Required</b>	<15mA

The cost of magnetoelastic torque sensors increase with the available capacity of the particular system. Magnetoelastic sensors are available in two types. Type 1 measures the changes in magnetic circuit permeances produced by torque, in order to generate an output. The cost of Type 1 sensors vary depending on the required application. These sensors have a wide range of prices, from around \$1300 to over \$50 000 [6]. Type 2 observes the torque of the system and generates a corresponding magnetic field. Type 2

sensors are available for as low as \$10, since large volumes of the sensors are produced for an extensive range of applications [6].

Magnetoelastic load sensors operate based on similar principals as the torque sensors with the distinction that they are designed to specifically detect axial stresses. Currently, only a few companies including MDI manufacture this type of sensors. The sensors offered by MDI are durable, reliable, and do not require recalibration. The load sensor specifications are provided in TABLE VII [7].

**TABLE VII  
MDI LOAD SENSOR SPECIFICATIONS [7]**

<b>Range</b>	<b>&lt;1 lbs to 20 tons</b>
<b>Resolution</b>	0.25 lbs to 1 lbs
<b>Accuracy</b>	0.5% to 1.0%
<b>Repeatability</b>	0.25% to 0.4%
<b>Response to Change</b>	1kHz to 20kHz
<b>Substrate</b>	6.0mm to 600mm
<b>Operating Temperature</b>	-40C to 180C
<b>Power Required</b>	<15mA

Figure 27 illustrates the complete circuitry and equipment required from initial torque or force measurement all the way to the calibration process. The system consists of a set of magnetoelastic sensors to detect the applied torque or force, a magnetic field sensor array to capture the sensor’s output, a signal conditioning circuit to refine the signal output, and a data acquisition system (DAQ) to produce the required data from the magnetic field output obtained from the previous devices.

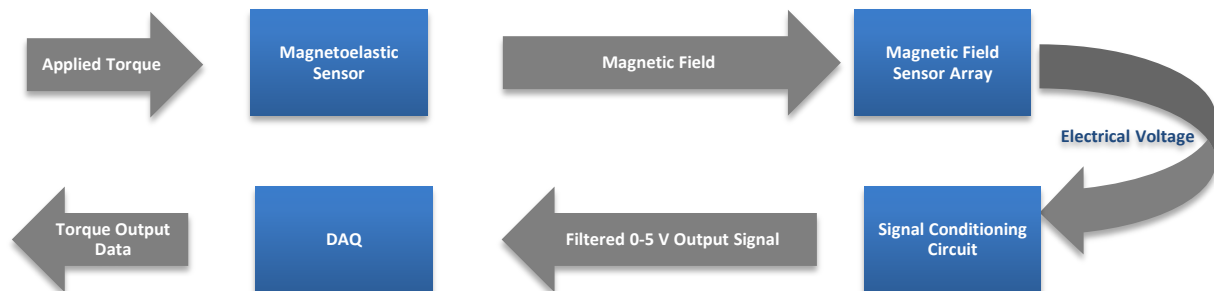


**Figure 27 Torque sensor system[10]**

A magnetic field sensor array is required to convert the output signal of the magnetoelastic sensors, which is of a magnetic nature, to an electric voltage signal usable in further stages of the system. Different kinds of these sensor arrays include flux gate sensors, Hall Effect devices, and magnetometers [6]. Hall-effect devices are very accurate and capable of taking the measurements from a remote area [8]. This results in reduced mechanical wear since they are not required to be mounted on the engine shaft. Hall devices are available from Allegro MicroSystems, inc. in different sizes and shapes with various specifications [9]. The calibrated linear Hall-effect sensors are available at a price of \$25.00 [9]. One disadvantage of Hall Effect devices and magnetometers is their sensitivity to temperature changes. This makes them less attractive compared to Flux gate type sensors which are capable of compensating for change in thermal conditions.

Since the output voltage of the magnetic field sensor array is very small, a system would be required to amplify the voltage to a value usable by the DAQ. This system is referred to as signal conditioning system. National Instruments offers a wide variety of such systems [11]. The NI 9211 signal conditioning system, is one example suitable for this application whose specifications are shown in Table VIII. This system is a thermocouple input module that produces an output that will be in turn used as the input to a DAQ.

**TABLE VIII**  
**SIGNAL CONDITIONING SYSTEM SPECIFICATIONS [11]**

		General
<b>Product Name</b>	NI 9211	
<b>Product Family</b>	Industrial I/O	
<b>Form Factor</b>	CompactDAQ , CompactRIO	
<b>Operating System/Target</b>	Windows , Real-Time	
<b>Measurement Type</b>	Temperature , Thermocouple , Voltage	
<b>Isolation Type</b>	Ch-Earth Ground Isolation	
<b>RoHS Compliant</b>	Yes	
<b>Signal Conditioning</b>	Cold-junction compensation	
Analog Input		
<b>Channels</b>	0 , 4	
<b>Differential Channels</b>	4	
<b>Resolution</b>	24 bits	
<b>Sample Rate</b>	14 S/s	
<b>Max Voltage</b>	80 mV	

<b>Maximum Voltage Range</b>	-80 mV , 80 mV
<b>Minimum Voltage Range</b>	-80 mV , 80 mV
<b>Physical Specifications</b>	
<b>Length</b>	9 cm
<b>Width</b>	2.3 cm
<b>I/O Connector</b>	Screw terminals
<b>Minimum Operating Temperature</b>	-40 °C
<b>Maximum Operating Temperature</b>	70 °C
<b>Minimum Storage Temperature</b>	-40 °C
<b>Maximum Storage Temperature</b>	85 °C

Finally, a DAQ is required in order to convert the voltage output to quantities of interest which are force and torque [12]. IOtech offers a number of DAQ's that are designed to be used in testing and measurement applications. One of these systems could potentially be used to produce the required data for engine testing. This provider also offers software to accompany these systems in order to obtain the data produced by the DAQ's. The IOtech 6222, which allows for accurate measurements, is a model that is available at the University of Manitoba. Specifications for the IOtech 6222 are given in Table IX. This system offers multiple channels, which would allow multiple sensors to be used simultaneously [12].

**TABLE IX  
IOTECH 6222 DAQ SPECIFICATIONS [5]**

<b>Input</b>	<b>Voltage, Thermocoupled</b>
<b>Channels</b>	12
<b>Resolution</b>	24-bit
	16-bit
<b>Included Software</b>	Encore interactive measurement
<b>Cost</b>	\$2299

[9] Another consideration in using magnetoelastic sensors is the potential interaction of the sensors. Since the intention is for the sensors to be in operation simultaneously, it is important to protect the sensors against interference. Magnetic field shielding can be used to prevent interference between non-contact sensors. Less EMF Inc. supplies magnetic field shielding in a wide variety of forms. Giron magnetic shielding film is an appropriate solution for this engine testing system. This film is thin, strong, and able to be shaped. It can also be

cut easily, and can be used for small applications. Therefore it is an ideal and versatile shielding solution for this application. The film cannot be exposed to direct sunlight, but it can operate in a wide range of temperatures. The specifications for the shielding are provided in TABLE X [13].

**TABLE X  
GIRON MAGNETIC SHIELDING SPECIFICATIONS [13]**

<b>Magnetic Field Range</b>	<b>0-1000Hz (AC or DC)</b>
<b>Operation Temperature Range</b>	32-122 °F
<b>Initial Permeability</b>	500
<b>Relative Permeability</b>	7000
<b>Saturation Induction</b>	2, 0 T
<b>Curie Temperature</b>	1364 °F
<b>Width</b>	25.5 in
<b>Thickness</b>	1 mm
<b>Weight</b>	3.5 kg/m
<b>Cost</b>	\$44.95/ft

The above shielding option is sold in very large quantities, therefore another smaller option to consider is the Metglas magnetic shielding film, which also sold by Less EMF Inc. This film is tough, yet it can be cut with scissors. It is also flexible and can be easily shaped. It can be used both indoors and outdoors, and is corrosion resistant. This film has been shown to reduce magnetic fields by almost 90%. The specifications for this shielding option are shown in Table XI [13].

**TABLE XI  
METGLAS MAGNETIC SHIELDING SPECIFICATIONS**

<b>Permeability</b>	<b>Over 1 000 000</b>
<b>Thickness</b>	0.00065 in
<b>Width</b>	1 in
<b>Cost</b>	\$2.50/ft

Through examining the operation of Magnetoelastic sensors, it was determined that, though accurate and reliable, these sensors are not suitable for this particular application.

As discussed earlier, magnetoelastic measurement approach would call for a number of subsystems to translate the measured input into the required data. When considered as one system, the total cost of the necessary components is quite large. Also, as described above, a polarized magnetoelastic material would need to interact directly with the engine shaft. Since the shaft of the Aero Design OS FX engine is not accessible, this particular method could not be implemented for this application. Temperature effects, mutual interference of the sensors' measurements, shielding, and lack of technical expertise are among other significant factors leading to this conclusion.

## C. TECHNICAL ANALYSIS AND VALIDATION

### 1. SIZING OF THE DEFLECTION ARM

An estimate of the torque developed by the engine is obtained from the engine manufacturer's power rating of 1.9 brake horsepower at 16000 rpm. Torque is calculated from the following relationship:

$$T = \frac{550P}{\omega} \quad (2)$$

Where

$T = \text{Torque in ftlbs}$

$P = \text{Horsepower}$

$\omega = \text{rotational speed of the engine in radians per second}$

This works out to a 0.62 ft-lbs or 7.5 in-lbs estimate of engine torque.

The deflection arm is essentially a cantilever beam with point loading applied to its tip. The equations defining the deflection and maximum stress developed for these conditions along with a rectangular beam cross-section are defined as follows.

$$\delta = \frac{4Fl^3}{Ebh^3} \quad (3)$$

$$\sigma = \frac{6Fl}{bh^2} \quad (4)$$

Where

$\delta = \text{beam tip deflection}$

$\sigma = \text{maximum stress}$

$F = \text{the load on the beam tip}$

$E = \text{modulus of elasticity of the beam material}$

$l = \text{beam length}$

$b = \text{beam width}$

$h = \text{beam thickness}$

The deflection arm is to be made of mild steel with minimum yield strength of 40ksi. Steel has the following property.

$$E = 30 \times 10^6 \text{ [psi]}$$

With the moment arm set to 1.5 inch, the beam length to 3 inches, and width 5/8 inch, the minimum thickness (h) is then calculated using Equation (4). A safety factor (SF) of 3 is used in recognition that torque may be greater under power at lower engine rpm and that torque is developed over half of each full revolution of the crankshaft, during the power stroke, so that peak torque is likely higher.

$$h = \sqrt[2]{\frac{6Fl}{b\frac{\sigma}{SF}}} = \sqrt[2]{\frac{6(5lb)3in}{\frac{5}{8}in(\frac{40}{3}ksi)}} = 0.104 \text{ inches} \quad (4a)$$

This corresponds to a thickness of 12 gauge steel.

Checking the deflection with Equation (3):

$$\delta = \frac{4Fl^3}{Ebh^3} = \frac{4(7.5lb)(3in)^3}{30000ksi(\frac{5}{8}in)(0.104)^3} = 0.038 \text{ inches} \quad (3a)$$

Deflection of 0.038 inches is less than 1/16<sup>th</sup> of an inch which is not significant. This would cause only 1.5 degrees of rotation of the engine which is reasonable. Therefore the deflection arm should be made out of a minimum sheet thickness of 12 gauge steel.

The rotational inertia of the engine will be simulated as a mass on the end of a cantilever beam to calculate the systems natural frequency.

The equation for natural frequency,  $w_n$ , of a slender cantilever beam of length,  $l$ , Modulus of elasticity,  $E$ , and second moment of area,  $I$ , with end mass,  $m$ , is defined below [1].

$$w_n = \sqrt{\frac{3EI}{ml^3}} \quad (5)$$

With  $m$  in  $\text{lbf-s}^2/\text{in}$

The engine firing frequency places a periodic forced vibration on the deflection arm. To prevent unstable resonance, the system natural frequency will be compared to the firing frequency under normal operation.

Assuming the natural frequency is lower than the operating frequency which is estimated to be 200 Hz firing frequency at 12000 rpm. As a rough estimate, the engine is treated as a thin shelled sphere of 1 inch radius. This gives a conservative estimate since the actual mass distribution is at a greater distance from the axis of rotation which would increase the moment of inertia,  $\ell$ , and lower the natural frequency,  $w_n$ . For a thin shelled sphere of mass  $M$  and radius  $R$ , the moment of inertia,  $\ell$ , is as follows.

$$\ell = \frac{2}{3}MR^2 \quad (6)$$

With the above values

$$\ell = \frac{2}{3}1.5\text{lb}(1\text{in})^2 = 1\text{lb}\text{in}^2$$

Mass  $m$  will be equated to moment of inertia  $\ell$  by

$$m = \frac{\ell}{(1.5\text{in})^2} \quad (7)$$

And the second moment of area  $I$  of a beam of rectangular cross-section is

$$I = \frac{1}{12}bh^3 \quad (8)$$

Combining equations (5), (6), (7), and (8), with the proper units, the natural frequency is then:

$$w_n = \sqrt{\frac{Ebh^3}{4\frac{\ell}{(1.5in)^2}l^3}} = \sqrt{\frac{30000ksi(\frac{5}{8}in)(0.104in)^3}{4\frac{1bin^2}{(1.5in)^2}\left(\frac{1}{32.2}\frac{lbfs^2}{ftlb}\right)\left(\frac{1}{12}\frac{ft}{in}\right)(3in)^3}} = \frac{412radians}{second} \text{ or } 66Hz$$

Since testing will be performed at a range of engine rpm greater than 4000 and the natural frequency is lower than 66Hz, the beam dimensions determined should be adequate for capturing the engine torque without resonance. Since the natural frequency is lower than the specified frequency, the above assumptions are correct.

## 2. SIZING OF THE THRUST SENSOR

In order to determine the size of the rod, the following procedure was used:

The relationship between the stress acting on the rod,  $\sigma$ , the strain observed in the rod,  $\epsilon$ , and the modulus of elasticity,  $E$ , of the rod material is known to be:

$$E = \frac{\sigma}{\epsilon} \quad (9)$$

The above equation can be rearranged to determine the maximum strain that is allowed to occur in the rod prior to plastic deformation,  $\epsilon_{max}$ , considering the yielding stress of the material,  $\sigma_{Yield}$ :

$$\epsilon_{max} = \frac{\sigma_{Yield}}{E} \quad (10)$$

The strain is also known to be a function of both the maximum deformation of the rod,  $\delta_{max}$ , and the original length of the rod,  $L$ :

$$\epsilon_{max} = \frac{\delta_{max}}{L} \quad (11)$$

In order to ensure that the deformed rod will not exceed the length of the system, the maximum allowable deformation can be calculated as follows:

$$\delta_{max} = \epsilon_{max}L \quad (12)$$

Since  $\sigma_{Yield}$  is known to be a function of the maximum applied load,  $P_{max}$ , and the minimum cross sectional area of the rod,  $A_{min}$ :

$$\sigma_{Yield} = \frac{P_{max}}{A_{min}} \quad (13)$$

This equation can be used in order to determine  $A_{min}$ :

$$A_{min} = \frac{P_{max}}{\sigma_{Yield}} \quad (14)$$

The diameter of the rod,  $D$ , can be determined from the equation of the cross-sectional area of the rod:

$$A_{min} = \frac{\pi D_{min}^2}{4} \quad (15)$$

Four different materials were considered as potential options for the rod: 7075-T6 aluminum, 6061-T6 aluminum, grade 5 titanium, and steel. Using a rated load of 25 lb, the required rod size was determined for each of the materials. The weight,  $W$ , of each of the rods were also calculated by taking the material densities,  $\rho$ , into account. The results are shown in the following Table XII, for a rod length of 6 in. Since the linear guide was of a predetermined length, the length of the rod was chosen by subtracting the length of the torque section.

**TABLE XII  
SIZING OF THE THRUST ROD**

	<b>7075-T6 Aluminum</b>	<b>6061-T6 Aluminum</b>	<b>Grade 5 Titanium</b>	<b>Steel</b>
<b><math>\sigma_{Yield}</math> (psi)</b>	73000	37000	125000	45000
<b>E (psi)</b>	10400000	10000000	17000000	29700000
<b>P (lbm/in<sup>3</sup>)</b>	0.102	0.0975	0.162	0.284
<b><math>\epsilon_{max}</math></b>	0.0070	0.0037	0.0074	0.0015
<b><math>\delta_{max}</math> (in)</b>	0.04	0.02	0.04	0.01
<b><math>A_{min}</math> (in<sup>2</sup>)</b>	0.0003	0.0007	0.0002	0.0006
<b><math>D_{min}</math> (in)</b>	0.02	0.03	0.02	0.03
<b>W (lb)</b>	0.08	0.15	0.08	0.36

The rod will also be threaded at the end and be fastened to the engine platform. A diameter of a quarter inch will be used which will be more than sufficient to meet the requirements.

This rear wall is sized to ensure that it will remain rigid when the axial rod is put into tension. The required was determined for each of the four materials. Using a width,  $b$ , of 7 inches, which is required for the test stand, and a stock material thickness of 0.125 inches, the required height of the plate,  $h$ , was determined using the following equation.

$$h_{min} = \left( \left( \frac{12}{48} \right) \frac{P_{max} b^3}{t E \delta_{max}} \right)^{\frac{1}{3}} \quad (16)$$

Table XIII below lists the calculated height for each of the four materials.

**TABLE XIII  
SIZING OF THE BACK PLATE**

	<b>7075-T6</b>	<b>6061-T6</b>	<b>Grade 5</b>	<b>Steel</b>
	<b>Aluminum</b>	<b>Aluminum</b>	<b>Titanium</b>	
<b><math>h_{min}</math> (in)</b>	2.54	2.58	2.16	1.79

Therefore the back plate of 3 inches high will be more than sufficient to minimize interference with the results.

### **3. LINEAR BEARING FRICTION TESTING AND ANALYSIS**

In the initial design of the test stand, linear bearings were identified as the thrust bearings to be used on the linear guides attached to the side plates. Looking at the manufacturer’s catalogue for the bearings, no information was provided for the static coefficient of friction. Therefore, it was required to assess the magnitude of the static friction in order to see if a significant amount of thrust is lost. Figure 28 illustrates the effect of the friction force.

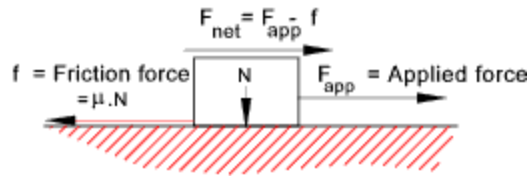


**Figure 28 Friction Force [14]**

The applied force,  $F_{app}$ , in the above Figure 28, is the actual thrust produced;  $N$  is the normal force between the object (linear bearing) and the surface (linear guide), and  $F_{net}$  is the net force. The effect of frictional forces is to reduce the sensitive of thrust measurement. This is measured by the strain gages mounted on the tethering rod in the test stand. The static friction force is evaluated using the following equation:

$$f = \mu_s \cdot N \quad (17)$$

Where  $\mu_s$ , is the static coefficient of friction and  $N$ , is the normal force between the surface and the object. From equation (17) it can be seen that for a high coefficient of friction, a big frictional force is created resulting in a smaller  $F_{net}$  in Figure 28. Therefore, it is very important to minimize the effect of friction as best as possible to obtain reliable measurements.

Using the facilities available in the Aero Design Team’s workshop at the University of Manitoba, the team carried out a test to determine the effect of the friction force produced by the linear bearings initially selected. Figure 29 shows the test set up.

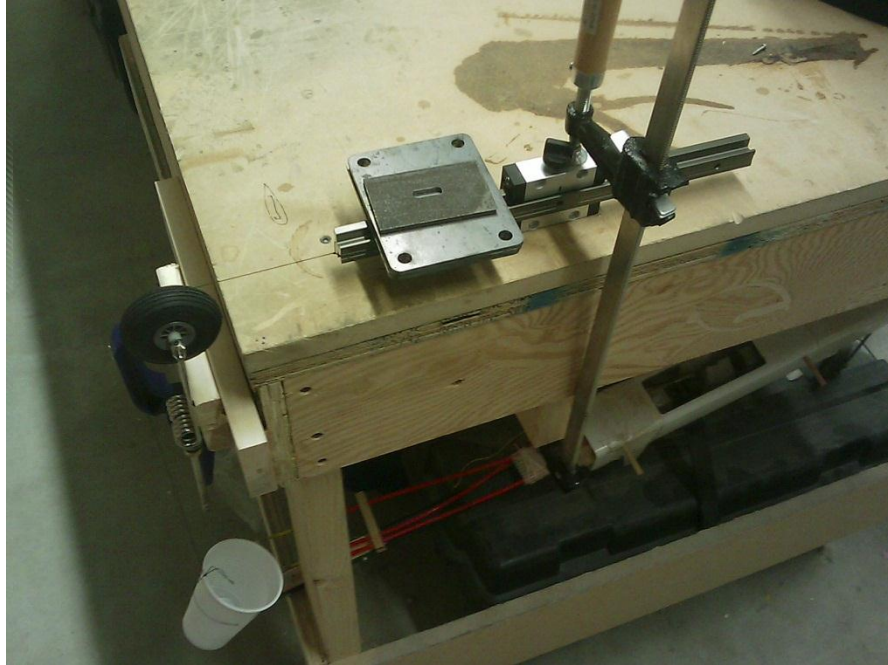


**Figure 29 Bearing Load Test Setup**

As shown, the linear bearing was fixed to the edge of a table using a C-clamp. A string was wrapped around the wheel, which was used as a pulley, and connected to the linear guide. A metal block weighing nearly 1.5 pounds was placed on the linear guide and fixed by tape to simulate the weight of the engine. Weight was gradually added to the cup hanging from the pulley until the linear bearing rail began to move through the bearing. The test was repeated several times and a friction force of nearly 1 to 1.2 pounds was recorded. Therefore, it was concluded that use of these linear bearings would result in a significant difference in the actual readings of the thrust since much of the thrust is being lost in overcoming the static friction of the linear bearings.

A better alternative is to use a roller contact type of linear bearing. Rolling bearings have high loading capacity and exhibit very little rolling friction and negligible sliding.

Many different types of roller bearings with various coefficients of friction exist. The current thrust ball linear bearings used for the test stand with coefficient of friction of  $f = 0.0013$ , have very low friction. This ensures minimal interference on the measurements [15].

#### 4. SIZING OF THE BEARING SHAFT

The bearing shaft is subjected to both a moment and a torque simultaneously. As well, there will be a stress concentration at the retaining ring, shoulder and the radial hole which the restraining pin is placed. The bending moment is exerted by the weight of the engine affixed to the one end of the shaft. This moment is relatively small therefore will be considered negligible in the determination of the size of the shaft. The torque is also relatively small, measuring 0.6 ft-lbs at maximum. Therefore the bearing shaft will be of sufficient size for the application and will remain rigid during the operation of the test.

#### 5. MEASUREMENT OF POWER AND THRUST

At the location of the strain gages on the deflection arm the torque can be determined using the following equations:

$$T = P * d_{arm} \quad (19)$$

$$\sigma = E\epsilon \quad (20)$$

$$\sigma = \frac{My}{I} = \frac{6P(L-a)}{bh^2} \quad (21)$$

$$P = \frac{E\epsilon bh^2}{6(L-a)} \quad (22)$$

$$T = \frac{E\epsilon bh^2 d_{arm}}{6(L-a)} \quad (23)$$

In the above equation, E represents the elastic modulus,  $\epsilon$  is the strain measured by the gage, b is the width of the deflection beam, h is the cross sectional height of the deflection beam,  $d_{arm}$  is the distance from the load to the rotation center of the engine, L is the length of the deflection beam and a is the position of the strain gage along the length of the beam measured from the fixed end. Each of these parameters is specified in the previous section. To convert the torque into a power measurement, the following equation must be applied, where omega represents the rotational speed of the propeller:

$$Q = \frac{\omega T}{550} \quad (24)$$

Measurement of thrust is accomplished using the following relationships:

$$\sigma = E\epsilon \quad (20)$$

$$\sigma = \frac{P}{\pi * r^2} \quad (25)$$

$$P = E\epsilon\pi r^2 \quad (26)$$

In the above equations P represents the thrust, E is the elastic modulus of the shaft, epsilon is the measured strain and r is the radius of the shaft.

## D. PART DRAWINGS

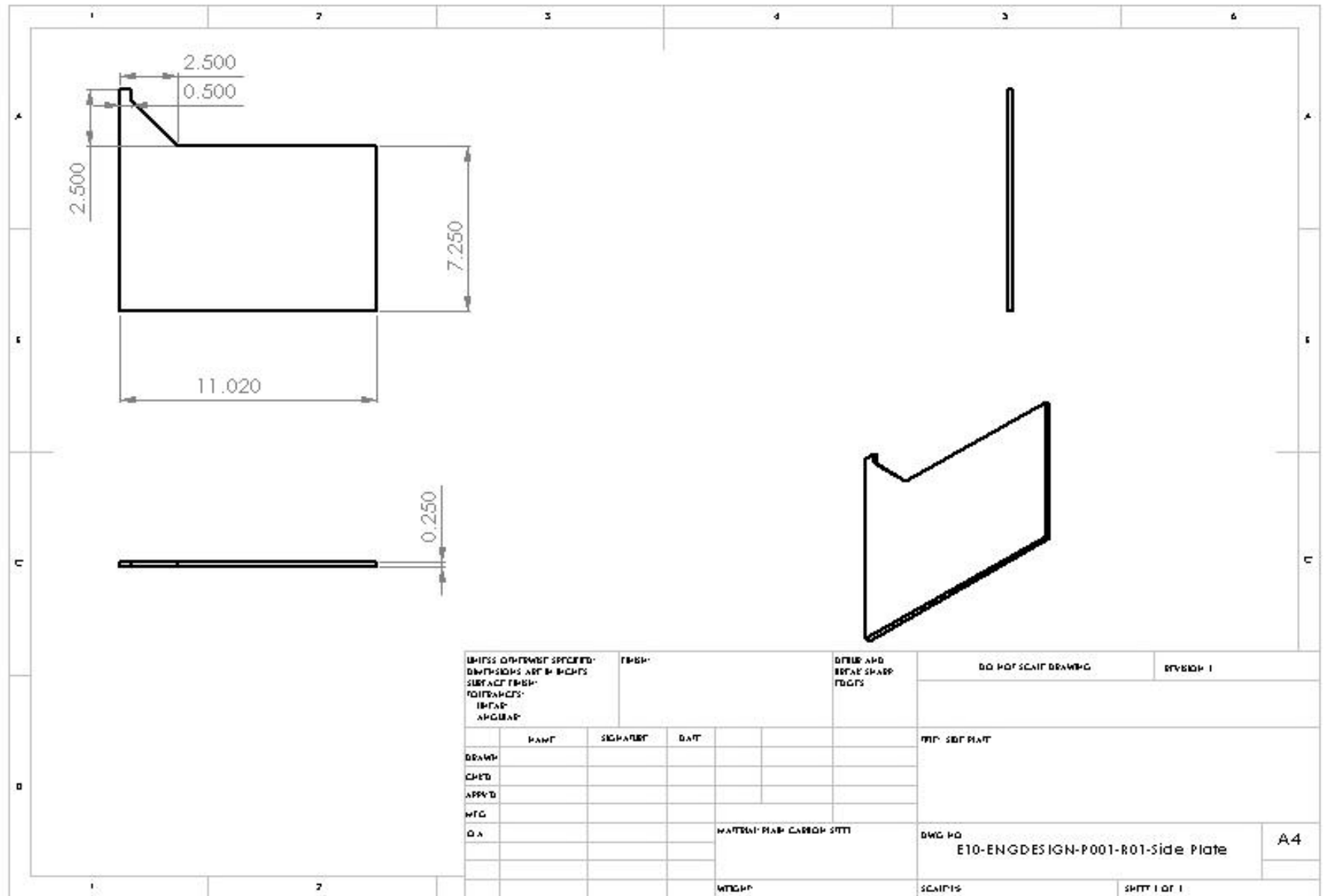


Figure 30 Side plate drawing

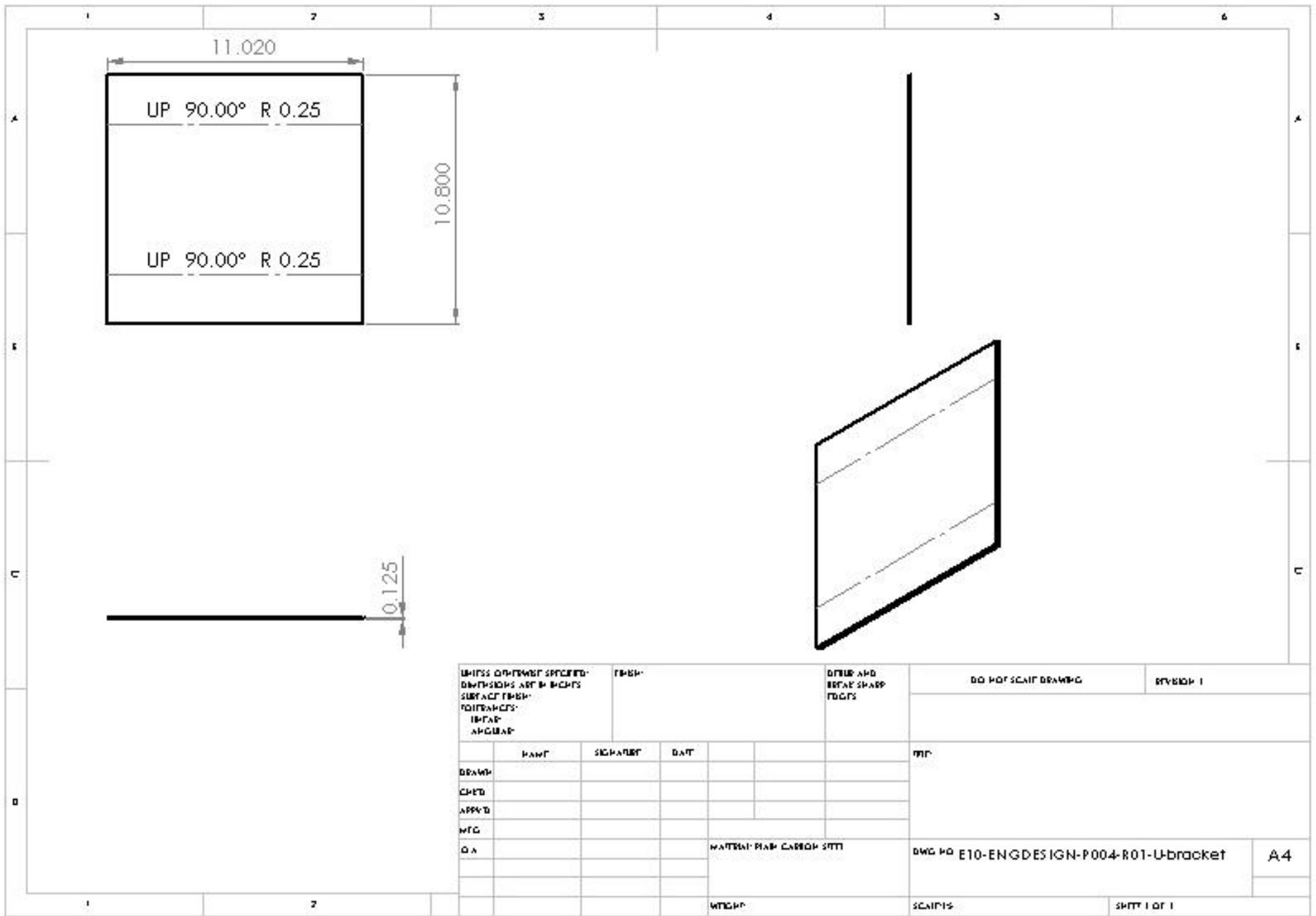


Figure 31 U-channel bracket drawing

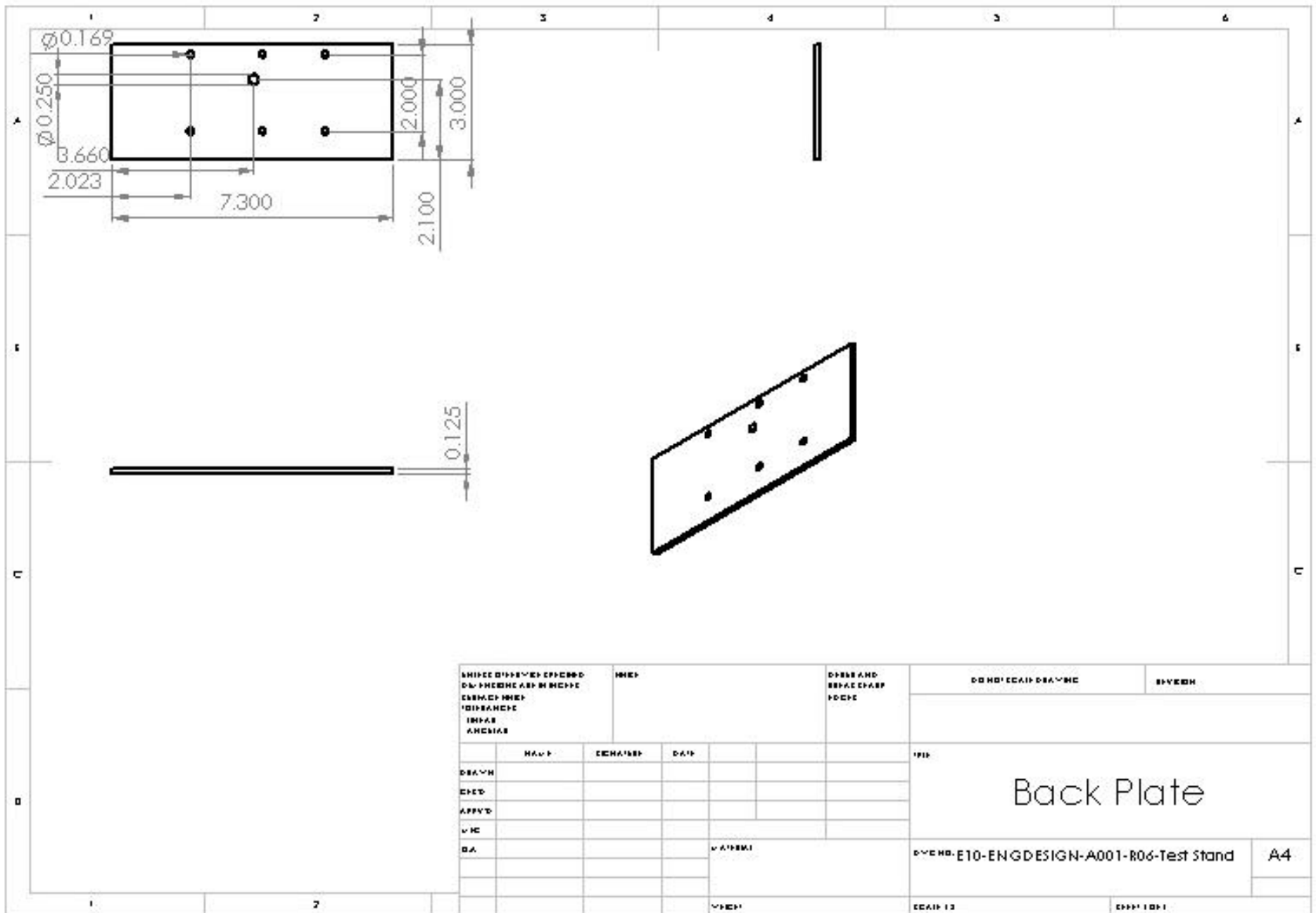


Figure 32 Back plate drawing



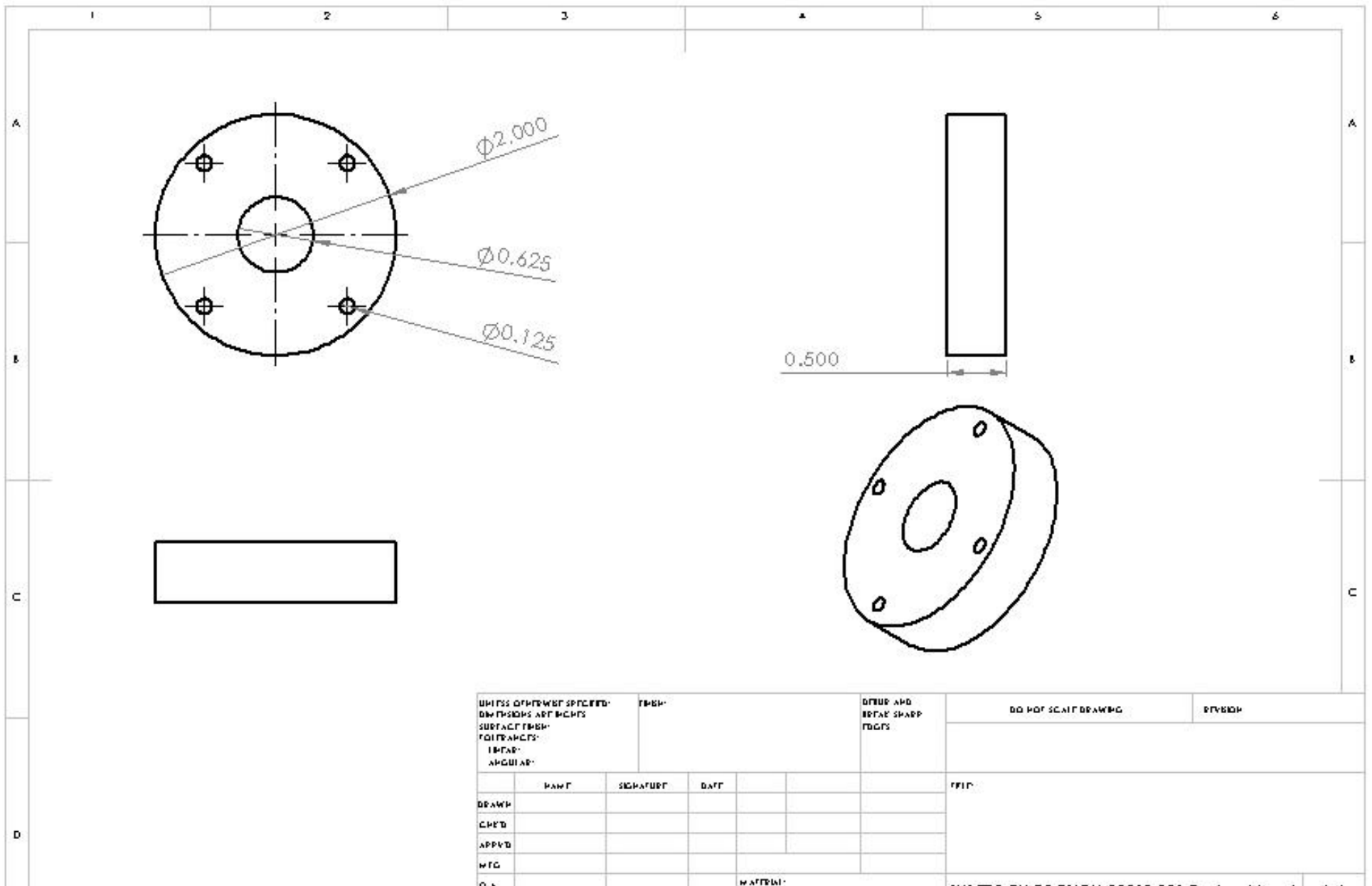


Figure 34 Engine mount drawing

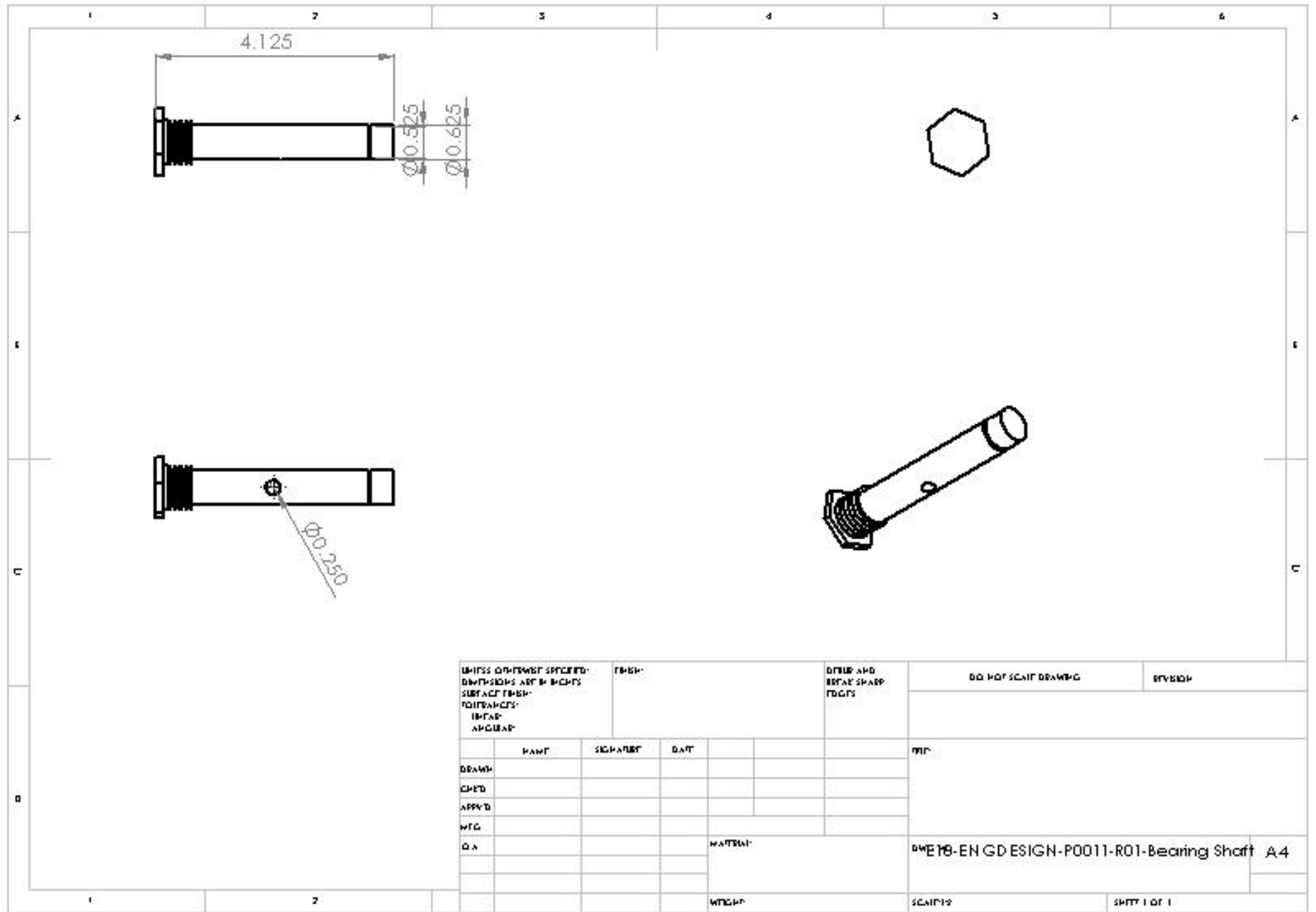


Figure 35 Bearing shaft drawing





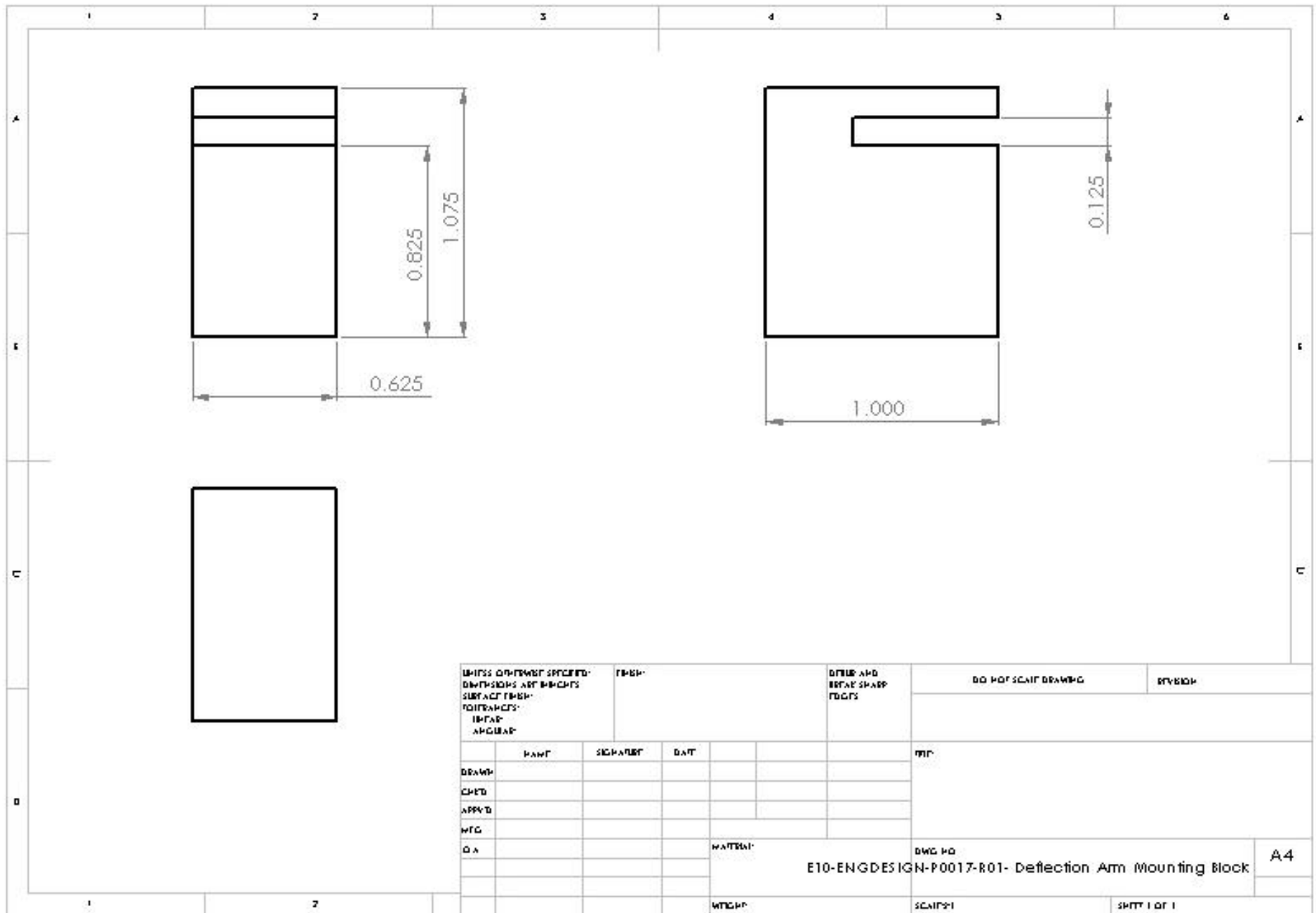


Figure 38 Deflection arm mounting block drawing

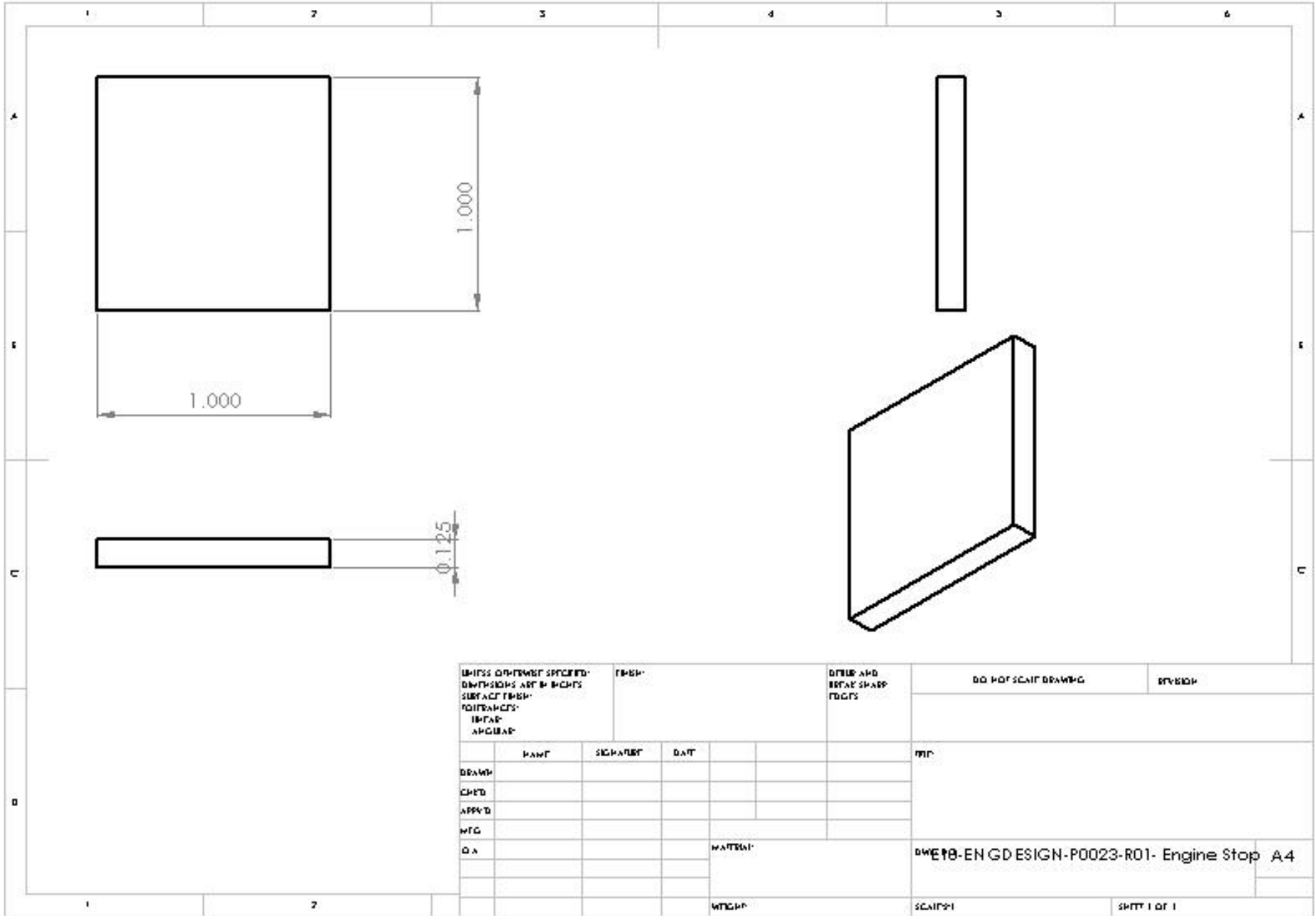


Figure 39 Engine stop drawing

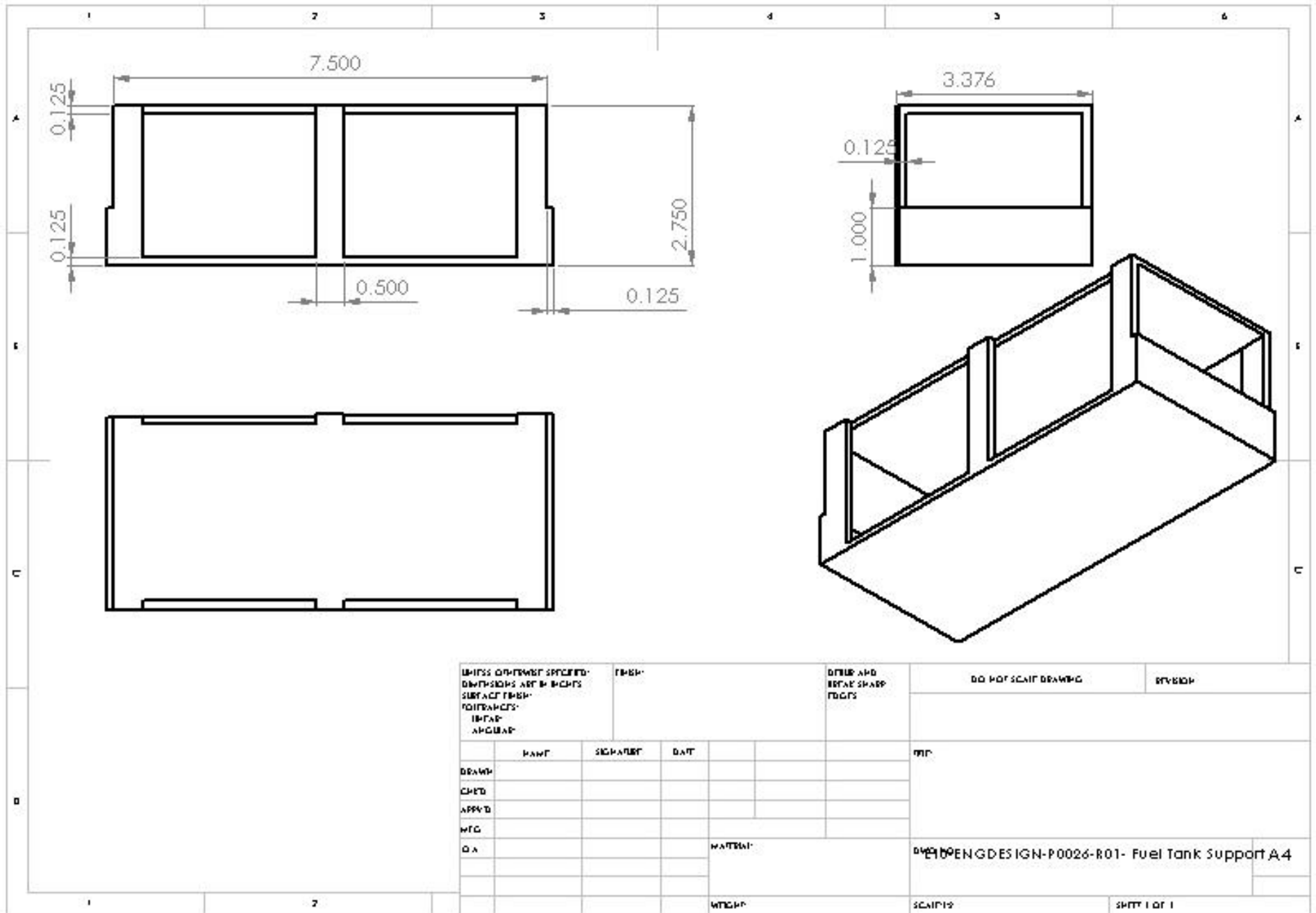


Figure 40 Fuel tank support drawing

## E. MANUFACTURING AND ASSEMBLY

To maintain consistency, metric fasteners are specified for the test stand, since several purchased components (linear bearings, pillow bearings, engine mounting fasteners etc.), require metric fasteners. Access is given to fasteners locations for easy assembly of the test stand. The pivot shaft however is made difficult to remove by using a snap ring. This prevents its unintended removal.

Manufacturability has been an important consideration for components of the test stand. Since only one test stand will be built, processes with high initial cost regardless of processing cost per part are unfavourable. Rolling metal into shape is one of the most basic and cost effective post-refinement processes. Sheet metal is produced by a rolling process. Sheet metal is used extensively for the test stand frame. Sheet metal, since it is a relatively inexpensive and versatile form. In our design, edges are bent to increase component stiffness and produce surfaces to which other parts may be fastened by bolts instead of using an intermediate bracket.

Different manufacturing processes are able to achieve different tolerances. Where greater accuracy is needed, a milling machine will be used. For example the torque arm hole pattern will need to be fairly accurate since calculations of torque depend on its length. Table XIV highlights the manufacturing processes involved for a few of the test stand components. Since this test stand will be a one-time production, accuracy must be ensured.

**TABLE XIV  
MANUFACTURING PROCESSES USED FOR VARIOUS TEST STAND COMPONENTS**

Lathe	<b>Milling machine</b>	<b>Band Saw</b>	Bending Brake
Pivot shaft	<b>Deflection arm</b>	<b>Frame</b>	Frame
Engine mounting plate	<b>mounting blocks</b>		
	frame		

## F. COST ANALYSIS

The detailed cost breakdown of the test stand design is provided in TABLE XV.

**TABLE XV  
DETAILED COST ANALYSIS**

<b>Item</b>	<b>Part Description</b>	<b>Part Number</b>	<b>QTY</b>	<b>Material Cost</b>	<b>Machining Cost</b>	<b>Unit Cost</b>	<b>Total Cost</b>
1	Back Brace	E10-P006	2	\$10.00	\$60.00	\$70.00	\$140.00
2	Back Plate	E10-P005	1	\$12.15	\$60.00	\$72.15	\$72.15
3	Bearing Shaft	E10-P0011	1	\$30.00	\$60.00	\$90.00	\$90.00
4	Deflection Arm	E10-P0016	1	\$1.35	\$60.00	\$61.35	\$61.35
5	Deflection Arm Mounting Block	E10-P0017	1	\$1.00	\$60.00	\$61.00	\$61.00
6	Engine Mounting Plate	E10-P0010	1	\$5.00	\$40.00	\$45.00	\$45.00
7	Engine Platform	E10-P007	1	\$32.40	\$60.00	\$92.40	\$92.40
8	Engine Stop	E10-P0023	2	\$1.00	\$60.00	\$61.00	\$122.00
9	Fuel Tank	DUB424	1	\$0.00	\$0.00	\$7.00	\$7.00
10	Fuel Tank Support	E10-P0026	1	\$5.00	\$30.00	\$35.00	\$35.00
11	Limiter Pin	E10-P0024	1	\$10.00	\$60.00	\$70.00	\$70.00
12	Linear Bearing System	E10-A003	2	\$0.00	\$0.00	\$224.70	\$224.70
13	Load Cell	MLP-10	1	\$0.00	\$0.00	\$300.00	\$300.00
14	Pillow Block Bearing Assembly	KSTI-10	2	\$0.00	\$0.00	\$25.00	\$50.00
15	Retaining Ring	1460-75	1	\$0.00	\$0.00	\$50.00	\$50.00
16	Side Plate	E10-P001	2	\$155.40	\$60.00	\$215.40	\$430.80
17	Throttle Linkage	E10-P0029	1	\$0.00	\$0.00	\$5.00	\$5.00
18	Throttle Servo	S185	1	\$0.00	\$0.00	\$50.00	\$50.00
19	Throttle Servo Arm	E10-P0031	1	\$0.00	\$0.00	\$5.00	\$5.00
20	Throttle Servo Mount	E10-P0032	1	\$5.00	\$40.00	\$45.00	\$45.00
21	Thrust Shaft	E10-P0014	1	\$5.00	\$60.00	\$65.00	\$65.00
22	Thrust Strain Gauge	CEA-13-240UZ-120	2	\$0.00	\$0.00	\$50.00	\$100.00
23	Torque Arm	E10-P0015	2	\$1.00	\$60.00	\$61.00	\$122.00
24	Torque Strain Gauge	CEA-13-240UZ-120	2	\$0.00	\$0.00	\$50.00	\$100.00
25	U-Bracket	E10-P004	2	\$69.30	\$60.00	\$129.30	\$258.60
26	Fasteners	N/a	N/a	N/a	N/a	N/a	N/a
27	IOTECH 6224	IOTECH 6224	1	N/a	N/a	\$2299	\$2299
<b>TOTAL</b>							<b>\$4896.00</b>

The detailed cost analysis, after taking into consideration the resources and sponsors available to the Aero Team, is presented in TABLE XVI.

**TABLE XVI  
UPDATED DETAILED COST ANALYSIS**

<b>Item</b>	<b>Part Description</b>	<b>Part Number</b>	<b>QTY</b>	<b>Material Cost</b>	<b>Machining Cost</b>	<b>Unit Cost</b>	<b>Total Cost</b>
1	Back Brace	E10-P006	2	\$0.00	\$0.00	\$0.00	\$0.00
2	Back Plate	E10-P005	1	\$0.00	\$0.00	\$0.00	\$0.00
3	Bearing Shaft	E10-P0011	1	\$0.00	\$0.00	\$0.00	\$0.00
4	Deflection Arm	E10-P0016	1	\$0.00	\$0.00	\$0.00	\$0.00
5	Deflection Arm Mounting Block	E10-P0017	1	\$0.00	\$0.00	\$0.00	\$0.00
6	Engine Mounting Plate	E10-P0010	1	\$0.00	\$0.00	\$0.00	\$0.00
7	Engine Platform	E10-P007	1	\$0.00	\$0.00	\$0.00	\$0.00
8	Engine Stop	E10-P0023	2	\$0.00	\$0.00	\$0.00	\$0.00
9	Fuel Tank	DUB424	1	\$0.00	\$0.00	\$0.00	\$0.00
10	Fuel Tank Support	E10-P0026	1	\$5.00	\$0.00	\$5.00	\$5.00
11	Limiter Pin	E10-P0024	1	\$0.00	\$0.00	\$0.00	\$0.00
12	Linear Bearing System	E10-A003	2	\$0.00	\$0.00	\$0.00	\$0.00
13	Load Cell	MLP-10	1	\$0.00	\$0.00	\$0.00	\$0.00
14	Pillow Block Bearing Assembly	KSTI-10	2	\$0.00	\$0.00	\$50.00	\$100.00
15	Retaining Ring	1460-75	1	\$0.00	\$0.00	\$50.00	\$50.00
16	Side Plate	E10-P001	2	\$0.00	\$0.00	\$0.00	\$0.00
17	Throttle Linkage	E10-P0029	1	\$0.00	\$0.00	\$5.00	\$5.00
18	Throttle Servo	S185	1	\$0.00	\$0.00	\$50.00	\$50.00
19	Throttle Servo Arm	E10-P0031	1	\$0.00	\$0.00	\$5.00	\$5.00
20	Throttle Servo Mount	E10-P0032	1	\$0.00	\$0.00	\$0.00	\$0.00
21	Thrust Shaft	E10-P0014	1	\$0.00	\$0.00	\$0.00	\$0.00
22	Thrust Strain Gauge	CEA-13-240UZ-120	2	\$0.00	\$0.00	\$0.00	\$0.00
23	Torque Arm	E10-P0015	2	\$0.00	\$0.00	\$0.00	\$0.00
24	Torque Strain Gauge	CEA-13-240UZ-120	2	\$0.00	\$0.00	\$0.00	\$0.00
25	U-Bracket	E10-P004	2	\$0.00	\$0.00	\$0.00	\$0.00
26	Fasteners	N/a	N/a	N/a	N/a	N/a	N/a
<b>TOTAL</b>							<b>\$240.00</b>

For many industrial design projects, a breakeven analysis is performed to determine when an organization will begin to make a profit from the design that they have implemented.

The breakeven point occurs when the company has earned enough money to cover the expenditures required to design and construct their product. In the case of this particular project, since the University of Manitoba SAE is a not for profit, student run organization, there will not be a point when this design begins to produce returns in terms of profit.

Since the design will allow the team to obtain important performance data which will allow them to more accurately predict the performance of their aircraft design, the team anticipates that the engine test stand will contribute to an improved competition score. With better performance at competition, comes potential opportunity for future sponsors, which would contribute to the funding available to the Aero Design Team.

## G. DETERMINATION OF TARGET SPECIFICATIONS

The torque and rotational speed specifications as listed in table II of section I are derived from the engine specifications. Essentially the torque is directly related to the power and rotational speed through the following equation:

$$T = \frac{550P}{\omega} 12 [in * lb]$$

The maximum possible power, P, and rotational speed which are both specified in table XVII are inserted into the above equation and the maximum torque can be determined.

**TABLE XVII**  
**O.S. FX ENGINE SPECIFICATIONS [4]**

<b>Characteristic</b>	<b>Specification</b>
<b>Weight</b>	19.42 oz
<b>Fuel</b>	10% Nitro Methane
<b>Displacement</b>	0.601 in <sup>3</sup>
<b>Output Power</b>	1.9hp @ 16000 RPM
<b>RPM range</b>	2000-17000

The operating thrust range comes from experimental data performed by the aero design team in 2008. The engine was rigged onto a skateboard with a data acquisition system mounted to the skateboard. A pitot tube was installed above the propeller to measure the forward aircraft speed. The engine was then started and allowed to travel along a runway. The mass of the system was recorded and the velocity plot was differentiated with respect to time to learn the acceleration of the system. The thrust was then calculated using the following equation:

$$F_T = m * a$$

A plot of the thrust as a function of forward aircraft speed is presented in Figure 41.

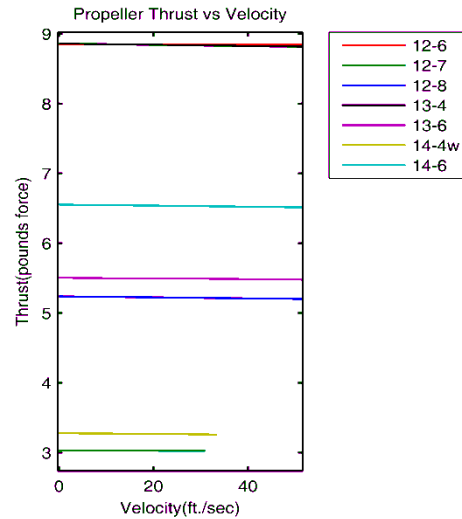


**Figure 41 Propeller thrust versus aircraft velocity [16]**

This procedure was repeated for the series of propeller diameters and pitches as shown above. Figure 30 shows that the maximum thrust obtainable for the O.S. 0.61 FX MAX engine is 9 pounds of thrust. Unfortunately the data obtained by the 2008 aero design team did not consider the effects of ambient weather conditions. Therefore the data is only used to generate a potential operating range for the thrust measured.

The propeller diameter and pitch specifications are also derived from the analysis presented above. A suitable range of propellers ranging from 11 inches in diameter and 14 inches in diameter are shown in figure 30 above to be a good starting point.

The airspeeds indicated are derived from data analysis performed by the 2011 aero design team where data acquisition systems were installed into the production aircraft. The aircraft was moderately loaded and the airspeed was recorded through the use of an installed pitot tube on the aircraft. From the data acquired, the largest velocity obtained was 75 feet per second. Therefore a range of 0-75 feet per second was considered adequate.

The engine operating temperature and noise were obtained from independent testing of the system during operation at competition.

Finally, the ambient conditions represent the full range of temperature conditions that the aircraft may be subjected to during competition. The system may operate outside of these conditions, but since the primary goal is to obtain results which will aid the team at competition, the system is calibrated to run in the conditions specified.

## H. ENGINE TACHOMETER SPECIFICATIONS

The engine tachometer will be utilizing an NPN photo transistor. The conductivity of the transistor is determined by the light level. The optical sensor sees the alternating levels of light between 0.7V and 5V or light and dark. Bias is removed using a series of capacitors and resistors. The output is then fed into a SN74393 4 bit counter. The counter represents the number of pulses seen since the system was last reset. The count is then fed into a SN74374 8-bit edge triggered latch, which captures the counts at set interval of time specified by the operator. The outputs of the latch are then fed into an SN74154 a 4-to-16 decoder which is then output to a data recording system[17]. The circuit is represented in the schematic presented in figure 42.

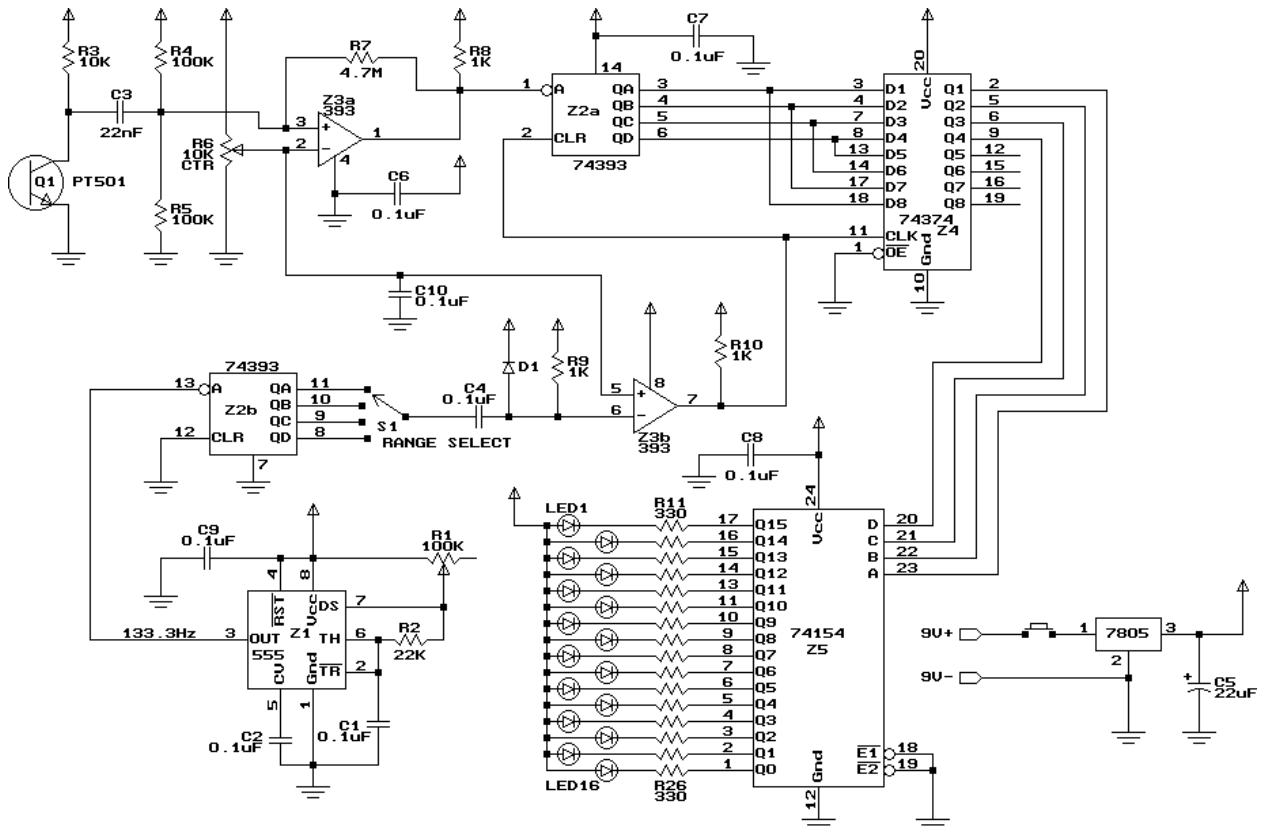


Figure 42 Schematic of the phototransistor based tachometer [17]

A full list of parts and specifications is presented in table XVIII. The full range of operation is between 0 and 16000 rpm.

**TABLE XVIII**  
**SPECIFICATIONS OF THE PHOTOTRANSISTOR TACHOMETER [17]**

<b>Part</b>	<b>Description</b>
<b>R1</b>	100 kohm trimmer potentiometer
<b>R2</b>	22 kohm ¼ W resistor
<b>R3</b>	10 kohm ¼ W resistor
<b>R4, R5</b>	100 kohm ¼ W Resistor
<b>R6</b>	10 kohm trimmer potentiometer
<b>R7</b>	4.7 Mohm ¼ W resistor
<b>R8,R9,R10</b>	1 kohm ¼ W Resistor
<b>R11-R26</b>	330 ohm ¼ W Resistor
<b>C1, C2, C4, C6-C10</b>	0.1 microFerad capacitor
<b>C3</b>	22 nanoFerad capacitor
<b>C5</b>	22 microFerad electrolytic capacitor
<b>D1</b>	1N914 Diode
<b>S1</b>	SP4T rotary Switch
<b>Z1</b>	LM555 Timer
<b>Z2</b>	SN74393 dual 4-bit counter
<b>Z3</b>	LM393 dual voltage comparator
<b>Z4</b>	SN74373 8-bit edge triggered latch
<b>Z5</b>	SN74154 4 to 16 line decoder
<b>VR1</b>	7805 5V 1A regulator
<b>Q1</b>	PT505 phototransistor
<b>LED1 – LED 16</b>	T-1 red LED 1.7-1.9V @ 10mA

## I. AMBIENT ENVIROMENTAL CONDITION SENSOR SPECIFICATIONS

The ambient condition sensor is a combination of a SCP1000 barometric pressure sensor, a SHT15 humidity sensor and a TEMA 6000 ambient light sensor. The system can transmit the information to a computer via USB or through Bluetooth wirelessly. The output is a serial string at 9600 bps at 1 reading per second. An example output from the device is as follows: #21.81,081.28,026.5,079.7,083534,918,0,000001\$. The first number is the humidity, the second is the temperature in Fahrenheit, the third is the temperature in Celsius, the fourth number is the temperature in Farenheit, the fifth number is the pressure in pascals, the sixth number is the light level in lumens, the seventh number is the battery level and the last number is the record number which will increment once per second.

The system can be powered from a USB port, drawing 5 V, or it can be powered from a 4-12 V external power supply such as a solar cell. The current draw when active is 35 mA. A full schematic of the circuit is shown in figures 43 and 44.

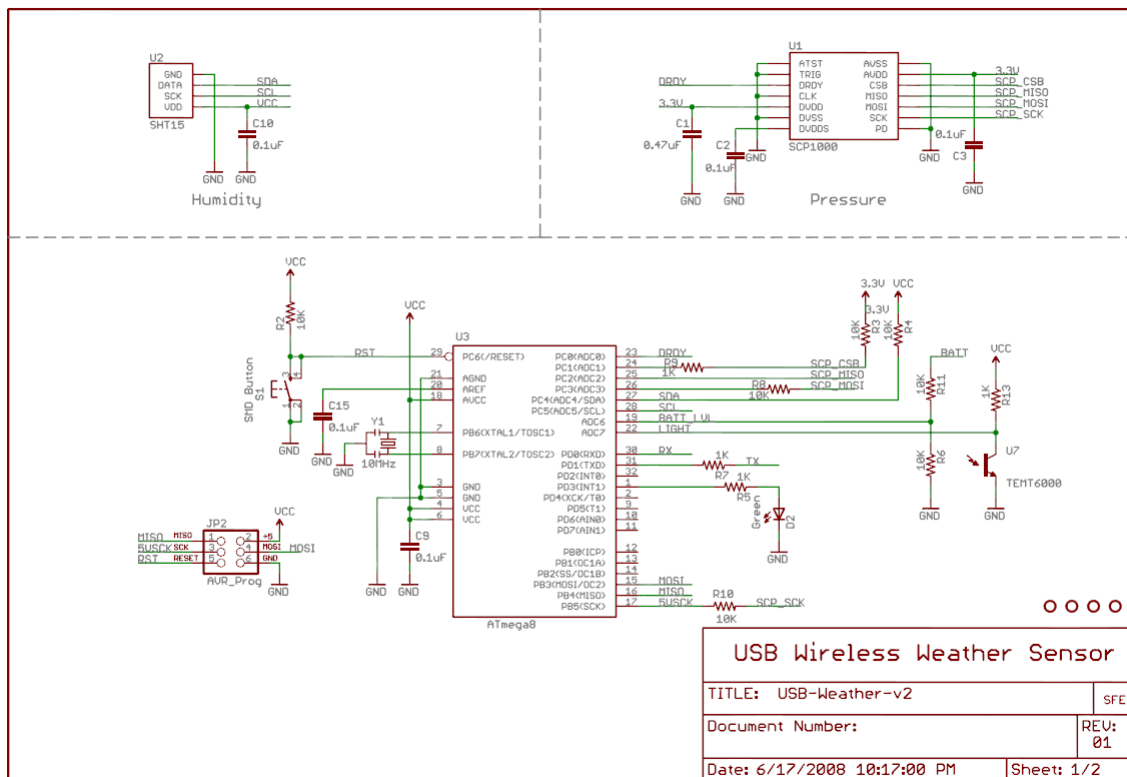


Figure 43 Schematic of the weather sensor[18]

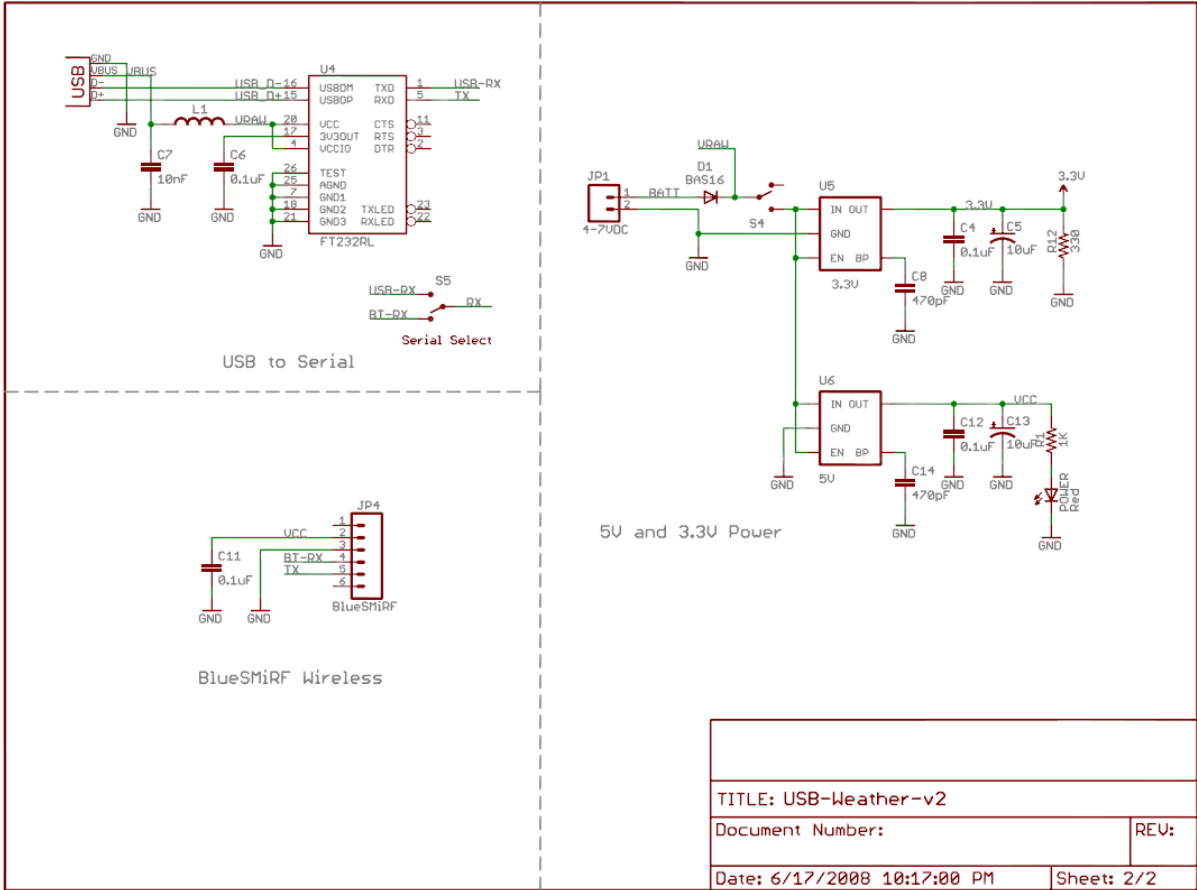


Figure 44 Schematic of the weather sensor[18]